ANALYSIS OF CONCRETE SUBSURFACE CRACKS USING ELASTIC R-WAVE METHOD

SAMANTHA AW JIA YING

A project report submitted in partial fulfilment of the requirements for the award of Bachelor of Engineering (Honours) Civil Engineering

Lee Kong Chian Faculty of Engineering and Science
Universiti Tunku Abdul Rahman

April 2021

DECLARATION

I hereby declare that this project report is based on my original work except for citations and quotations which have been duly acknowledged. I also declare that it has not been previously and concurrently submitted for any other degree or award at UTAR or other institutions.

Signature : 

Name : Samantha Aw Jia Ying

ID No. : 1603579

Date : 12th April 2021

APPROVAL FOR SUBMISSION

I certify that this project report entitled **"ANALYSIS OF CONCRETE SUBSURFACE CRACKS USING ELASTIC R-WAVE METHOD"** was prepared by **SAMANTHA AW JIA YING** has met the required standard for submission in partial fulfilment of the requirements for the award of Bachelor of Engineering (Honours) Civil Engineering at Universiti Tunku Abdul Rahman.

Approved by,

Signature : 

Supervisor : Dr. Lee Foo Wei

Date : 16/04/2021

ACKNOWLEDGEMENT

I want to express my sincere gratitude to several individuals and organizations for providing the platform and resources throughout my research study. First, I would like to express my sincere appreciation to my Final Year Project Supervisor, Dr. Lee Foo Wei, for the patience and guidance throughout my research study.

Next, I would like to express my sincere thanks to University Tunku Abdul Rahman for providing the facilities and resources for this research study. I am also grateful to thank my senior, Liew Chi Hoe, who guided me in analyzing results.

Last but not least, this final year project had enhanced my knowledge and understanding of the Rayleigh wave-based non-contact method, which can aid in the concrete quality assessment and helps in my future career.

ABSTRACT

Concrete often plays a vital role in the construction industry. The usage of concrete ranges typically from buildings, pavements, retaining walls, bridges, and other structures. The concrete's tensile strength is only 10 % of its compressive strength. Thus, the reinforcement bar is introduced to resolve the low tensile strength characteristics of concrete. The subsurface cracks will form due to the corrosion of steel reinforcement. It will continue to propagate and creating a horizontal crack in the concrete. The formation of subsurface crack is not visible, and it will cause a sudden collapse of a structure. It is essential to detect the concrete's crack and carry out appropriate action or repair to avoid the sudden collapse. The formation of crack will accelerate water and chemical substance penetration into the concrete and decrease the concrete's strength. The non-destructive test (NDT) is a method that can carry out to examine the properties of a material without damaging it. Thus, Rayleigh wave-based non-contact method was adopted to study the correlations of Rayleigh wave properties on the concrete subsurface cracks. In this research study, 104 cases were conducted to analyze the concrete subsurface cracks with different diameters, the different depth, and the Rayleigh wave generated varies using different sizes of steel ball diameter.

TABLE OF CONTENTS

LIST OF TABLES

LIST OF FIGURES

LIST OF SYMBOLS / ABBREVIATIONS

T	Period, s.
λ	Wavelength, m.
f	Compressive strength, N/mm^2.
P	Maximum load, N,
A	Area of concrete specimen, mm^2.
A(%)	Percentage of attenuation, %.
A_x	Amplitude of the first sensor.
A_{x+1}	Amplitude of the subsequent sensor.
V	Velocity of propagation of Rayleigh wave, m/s.
L	Distance between two sensors, m.
t_2	Arrival time of Rayleigh wave in the first sensor, s.
t_1	Arrival time of Rayleigh wave in the subsequent sensor, s.
V(%)	Percentage difference of average propagation velocity, %.
V_{avg}	Average propagation velocity between sensors, m/s.
V_s	Propagation velocity of sound concrete, 361 m/s.

NDT	Non-destructive Test
NDE	Non-destructive Evaluation
SDT	Semi destructive test
DT	Destructive Test
UT	Ultrasonic Test
MT	Magnetic Particle Testing
P-wave	Primary wave/ Longitudinal wave
S-wave	Secondary wave/ Transverse wave
R-wave	Rayleigh wave
FMC SAFT	Full Matrix Capture Synthetic Aperture Focusing Technique
FDTD	Finite-Difference Time-Domain
OPC	Ordinary Portland Cement
ASTM	International Association for Testing Materials
FFT	Fast Fourier Transform

CHAPTER 1

INTRODUCTION

1.1 General Introduction

In the construction industry, concrete often plays a vital role while constructing a building. The usage of concrete ranges typically from buildings, pavements, retaining walls, bridges, and other structures. The raw materials made up of concrete include cement, fine aggregates, coarse aggregates, and water mixed with an appropriate amount and ratio. In some specific applications, admixtures will be added to the concrete to achieve particular properties when they cannot be achieved by changing the raw material's proportion.

Concrete is widely used in construction work. Although the tensile strength is low, it can sustain a high compressive strength. On average, the tensile strength of concrete is only 10 % of its compressive strength. Therefore, a reinforcement bar is introduced to increase tensile stress resistance and provide a high load-bearing capacity for concrete. Although the usage of a reinforcement bar can increase tensile strength resistance, sometimes, factors such as overloading, thermal expansion, and differential settlement will still affect the concrete's quality in which causing the concrete to cracks on its surface or subsurface. Surface cracks are visible cracks that form on the concrete surface, whereas subsurface cracks are the cracks that are not visible on the surface but forms inside the concrete.

It is essential to detect the concrete's crack and carry out appropriate action or repair to avoid the sudden collapse. The formation of crack will accelerate the penetration of water and chemical substance into the concrete and causes corrosion of the reinforcement bar, decreasing the concrete's strength.

A non-destructive test (NDT) is one method that can carry out to examine the properties of a material without damaging it. There are a few types of NDT, such as Ultrasonic Testing (UT), Thermography Method, and Magnetic Particle Testing (MT). NDT can be used to determine the strengths and detect the defects in concrete. It gives an accurate result at a moderate cost, making it a remarkable method to detect subsurface cracks.

1.2 Importance of the Study

Cracking in the concrete comes in many different forms. The formation of cracks in the concrete is very dangerous, especially subsurface crack. As subsurface crack occurs, it shows that the concrete's durability had decreased, and the concrete will have the risk of cracking or crushing. As compared with surface crack, subsurface crack is hidden in the concrete and not visible to the naked eyes until it breaks to the concrete surface. Therefore, it is essential to detect a subsurface crack in the concrete and propose repairing or other actions required. On the other hand, for reinforced concrete structures, a subsurface crack will cause the penetration of chemical substances or water into the concrete, accelerating concrete deterioration. It will further corrode the reinforcement bar and cut down the concrete structure's service life. The degree of danger of a subsurface crack can be seen in two aspects: crack depth and crack width. The deeper crack depth and a larger crack width indicating the structure will have a high tendency to have a sudden failure. In order to identify the subsurface crack, the Rayleigh wave-based non-contact method is adopted. It is a non-destructive test (NDT) that can test the current concrete condition without damaging the original specimen.

1.3 Problem Statement

Subsurface cracks are usually hidden under the concrete surface and form around the reinforcement bar. Non-destructive test (NDT) is the most suitable method to detect near-surface cracks. It is because subsurface cracks form under the concrete surface, and it is unable to see by naked eyes. With the aid of NDT, it allows us to monitor and visualize the defects in concrete without damaging the structure. Among all the different NDT types, the Ultrasonic non-contact method is the most suitable method to be adopted for this research. It requires the penetration of elastic waves through a medium to detect defects.

Rayleigh wave suits the most in detecting subsurface cracks in concrete among the different types of elastic waves. It can carry more energy which effectively decreases the geometric spreading and decreases the tendency of attenuation (Ghosh et al., 2018). Rayleigh wave is a type of surface wave where the wave's propagation is perpendicular to its travel direction in the vertical plane. By utilizing the Rayleigh wave, the location of subsurface cracks can be

determined, and the concrete's quality can be confirmed. Thus, remedial action can be carried out to extend the service life of the structure.

1.4 Aim and Objectives

This research study aims to study the characteristics and properties of the Rayleigh wave when propagating through a concrete specimen consisting of different types of subsurface crack with the Rayleigh wave-based non-destructive test using the non-contact sensors. The objectives of this research study are: -

1. To determine the Rayleigh wave characteristics' changes when propagating through a sound concrete and concrete with subsurface cracks.
2. To experimentally study the properties of Rayleigh wave when propagating through concrete with different diameters of subsurface cracks (100 mm, 200 mm, 300 mm, 400 mm, and 500 mm) and different depths of subsurface cracks (25 mm, 225 mm, 425 mm, 625 mm, and 825 mm), namely: -
    i. Attenuation
    ii. Velocity of propagation
    iii. Dominant frequency
3. To compare the waveforms result obtained when 10 mm, 15 mm, 20 mm, and 25 mm diameters of steel ball used to generate Rayleigh wave with different frequency.

1.5 Scope and Limitation of the Study

This research study will mainly focus on the analysis of subsurface cracks using the elastic Rayleigh wave method. Rayleigh wave-based non-contact method is adopted in this research study. It is a non-destructive testing (NDT) that requires elastic wave penetration through a medium to detect defects. The Rayleigh wave will be used to detect different types of subsurface crack depth and subsurface crack diameter among various types of elastic waves. It is because Rayleigh waves have high energy and relatively sensitive to defects. This method can detect a subsurface crack in different mediums such as aluminum, concrete, and

steel. This research study will be mainly focusing on the concrete subsurface crack.

There are some limitations to this research study. For the actual situation of a subsurface crack, it will not appear on the concrete's surface, and it is hard to determine the crack depth or crack pattern. An experiment called a four-point flexural test would be carried out to create a similar subsurface crack situation. But there are also limitations of this test as the crack occurs on the durability of the concrete. Thus, the crack depth is formed randomly, which may not be the expected depth to carry out the research study. The four-point flexural test is a more suitable method to create the subsurface crack in reinforced concrete. It is because the reinforcement bar in the concrete will provide higher tensile strength. For the concrete without reinforcement, the crack depth created might reach the opposite side of the concrete where the specimen will be spoilt, and it is a relatively costly and challenging approach. Therefore, the polystyrene boards were cut into different diameters to act as the artificial subsurface crack.

1.6 Contribution of the Study

From this research study, the results and outcome can effectively serve as a reference in the construction industry and contribute to further studies on cracking in concrete and applying the Rayleigh wave-based non-contact method. The formation of a subsurface crack in the concrete is a common issue in the construction industry. It is suggested to adopt the non-destructive test (NDT) in detecting a subsurface crack in concrete as the crack formation is not visible to naked eyes. At the same time, NDT will not damage the structure. Moreover, the analysis of subsurface cracks in different depths and diameters can effectively compare and understand how different types of cracks affect concrete strength. The different frequencies of Rayleigh wave were generated using different steel ball diameters. Thus, it can make a more precise comparison between different Rayleigh wave frequencies when it encounters different types of cracks.

1.7 Structure of Report

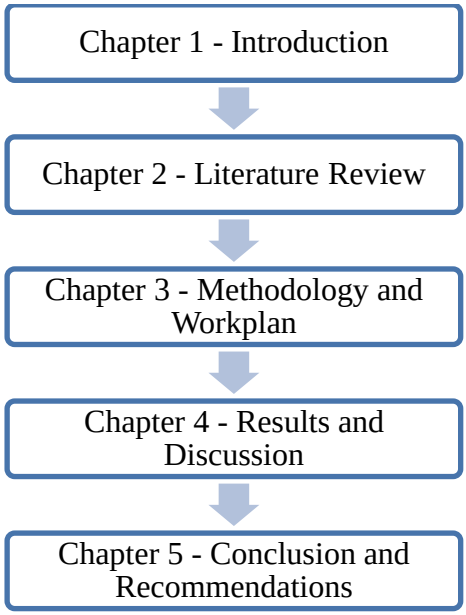

Figure 1.1: The structure of the report.

There are five chapters in this report. Chapter 1 provides a general introduction of concrete, subsurface crack and non-destructive tests (NDT). The importance of the study topic, problem statement, aims, and the objective was discussed. The study's scope and limitations and the contribution of the study were also elaborated in this chapter.

Chapter 2 is the literature review that concerns the cracking in concrete, can be categorized into the surface crack and subsurface crack. Some poor practices in the construction industry that leads to the cracking in concrete were elaborated. Moreover, this chapter discussed the methods in diagnosing buildings and building material, focusing on destructive testing (DT) and non-destructive testing (NDT). This topic also emphasizes contact and non-contact ultrasound testing, which requires the propagation of a wave through a medium. The parameters of waves and types of the wave were elaborated. The past research studies on the subsurface cracks were discussed in this chapter.

Chapter 3 talks about the methodology and work plan adopted in this research study. The Rayleigh wave-based non-contact method is adopted to determine the Rayleigh wave's effectiveness in detecting concrete subsurface crack. This chapter further discussed the raw material needed for the experiment, the process of raw material preparations, and the mixed proportions of raw

materials were provided. The detailed experimental analysis, such as the location of artificial subsurface cracks, the setup of experiments, and the waveform collection, were further discussed. The results of the compression strength test were also provided in this chapter.

For Chapter 4, the results obtained were tabulated in graphs and tables form. The discussions were made according to the results collected from the experimental analysis. The discussed topic includes the arrival time, the percentage of attenuation, the propagation velocity, and the dominant frequency of Rayleigh wave in different frequencies.

Finally, the final chapter concluded the results obtained to summarize the aim and objective stated. The recommendations were suggested to improve and enhance the experimental analysis for further studies on related topics.

1.8 Summary of the Chapter

This chapter gives a brief introduction to concrete, concrete usage in the construction industry, and the formation of subsurface cracks. NDT is an approach that can detect defects in material while not causing any damage to it. There are a few types of NDT, where Ultrasonic Testing (UT) is a type of NDT which use the propagation of wave to detect defects in a medium. Rayleigh wave is adopted as it has maximum energy made it sensitive to detect subsurface cracks. This study has one aim and three objectives to provide a better solution to detect near-surface cracks and to carry out further actions. There are also scope and limitations in this research study as there will be a problem in creating an actual subsurface crack. This research study can also effectively helps in further studies on the related topics.

CHAPTER 2

LITERATURE REVIEW

2.1 Introduction

Concrete established high strength and high durability performance to ensure a firm structure, but concrete cracking is the most common construction industry problem. The cracking of concrete is inevitable, but sometimes, people may think something wrong when cracks form on concrete. Although cracking of concrete is a common issue, not every formation of cracks on the concrete indicates that the quality had degraded. There are two types of cracks, namely surface crack, and subsurface crack. The easiest way to differentiate both cracks is to examine the concrete surface condition. Surface cracks always form on the concrete surface, and it penetrates the concrete. The subsurface cracks cannot be observed using naked eyes as it is formed inside the concrete until it slowly penetrates out to the surface. Many situations will cause concrete to crack. For example, it might be due to the rapid drying of concrete and excess water in the concrete mix. Thus, the concrete subsurface cracks' detection is relatively essential to determine the structure's degree of danger.

There are two methods to diagnose buildings and building material: the destructive test (DT) and the non-destructive test (NDT). First of all, DT is used to examine the compressive strength of concrete, which involves destroying the concrete specimen to determine its performance. Splitting tensile tests, concrete cube tests, and flexural strength tests are examples of DT. DT's most significant limitation is that it must wholly or partially destroy part of the structure to determine the particular structure's strength.

On the other hand, another test is the non-destructive test (NDT) which can determine the concrete quality without damaging the structure. Thermography test, Ultrasonic test (UT), and Magnetic Particle Testing (MT) are a few examples of NDT. In comparison to DT, NDT requires a person with professional skills to carry out the test. The total cost needed for NDT is also higher than DT. The result's accuracy for both DT and NDT is relatively the same. Some of the studies on the concrete structure's performance must be done

using NDT instead of DT, such as visualization of concrete subsurface and detection of cracks in concrete.

This research study will mainly focus on the detection of the subsurface crack in the concrete. Detection of the subsurface crack is to determine the quality of the existing structure. Therefore, it should be done without damaging the structure. The NDT chosen in this research study is the ultrasonic non-contact method, which requires penetration of elastic waves through the target structure to examine its quality. A few types of elastic waves are available, such as Longitudinal waves, Transverse waves, Rayleigh waves, and Love waves. Out of all the types of elastic waves, the Rayleigh wave was selected to detect the subsurface crack in this research study.

2.2 Cracking of Concrete

Cracking of concrete occurs when there are tension forces. For reinforced concrete structures, the maximum design crack width is 0.3 mm, as stated in Eurocode (EN BS: 1992). The crack width within the limit does not cause the structure's failure, provided that the bonding between the reinforcement bar and concrete is good. When the crack formed is larger than the tolerated limit, it will accelerate chemical substances and water to penetrate the concrete. It will further increase the tendency of the reinforcement bar to corrode and affects the concrete's service life. The steel reinforcement is designed to distribute the tensile forces through the bonding between concrete and steel bars. Cracking of concrete may occur before hardening, approximately 3 to 4 hours of concrete placing due to vibration and plastic shrinkage. It may also occur after the concrete's hardening process due to differential settlement, overloading, weathering action, and thermal expansion. Usually, cracking can be solved by injecting cement into the cracks to fill them up. However, in some conditions, provided that the crack width is too large, the structure's affected area should be demolished and reconstructed. When there are different concrete widths and patterns, different types of cracks will occur. Cracking comes in different depth or width, which needs to be controlled before the sudden failure of the structure happens. Cracking in concrete can be classified into two main groups, which are surface crack and subsurface crack. Sometimes surface cracks will happen, and it tends to penetrate the concrete and become subsurface crack.

2.2.1 Surface Crack

Surface cracks are the cracks that form on the concrete surface, which are visible to naked eyes. One can easily determine the quality of concrete by observing the surface of the structure. The surface cracks often happen in freshly placed concrete. The change in wind speed, the surrounding temperature, and humidity will increase the possibility of plastic shrinkage cracking. Plastic shrinkage will cause an early crack of concrete which is a hairline-like crack on the surface, and it will continue to penetrate in the concrete. This crack is due to an excess amount of water in the concrete mix. The high content of water cause segregation in the concrete, where aggregate and cement paste separates during concrete placing.

A drying shrinkage crack is one of the surface cracks caused by water loss during the hardening process. The loss of water from concrete leads to a change in volume, and stress will develop in the concrete. When the stress developed exceeds its tensile limit, the crack starts to form. Therefore, a proper mix design can be an exercise to reduce bleeding, thus preventing drying shrinkage.

2.2.2 Subsurface Crack

Subsurface crack is also known as the near-surface crack. The corrosion of the steel reinforcement bar causes the formation of concrete subsurface cracks. The formation usually starts from the reinforcement bar and propagates along connects with the crack nearby, forming a fracture plane (Li et al., 2007). The different concrete section detailing and reinforcement bar corrosion rate will affect the fracture plane's size. (Cady and Weyers, 1984) found out that the subsurface cracks caused by the corrosion of the reinforcement bar come in two conditions that are parallel to the rebar or inclined. When the concrete cover thickness is lesser than 25.4 mm, an inclined crack will occur. The parallel crack happens when the concrete cover thickness is greater than 31.8 mm. (Dagher and Kulendran, 1992) stated that cracks might forms between reinforcement bars when the arrangement is too closely packed to each other. In contrast, when the spacing between reinforcement bars is larger, the crack tends to penetrate upwards until reaching the concrete's surface. It will accelerate the concrete's deterioration because subsurface cracks allow chemical substances and water to

penetrate it, which will further affect the concrete's durability. Subsurface crack is not visible as it forms inside the concrete. It will take a couple of months or years for the subsurface cracks to penetrate to the surface to be visible.

Plastic shrinkage is one of the common causes of subsurface crack. As mentioned above, the subsurface crack usually forms around the reinforcement steel. During the concrete hardening process, fresh concrete tends to rest on the reinforcement bar, where the sudden change in cross-sectional thickness occurs (Chakravarthi, 2014). Subsurface cracks formed in the area near the reinforcement bar and concrete cover.

2.2.3 Poor Construction Practice that cause Cracking in Concrete

During the construction phase, workers tend to ignore the standard procedure of placing the concrete. To save cost and time, workers will proceed with the poor construction practice that may cause cracking in concrete and degrade the concrete strength. The action of adding water into the concrete mix often happens on-site to increase the workability of the concrete mix. However, when the water content increases, the tendency of drying shrinkage and plastic cracking will increase and further reduce the concrete strength. There is also a situation when too much water is added into the concrete mix and workers increase the cement content to offset it. This action will increase the temperature differential between the structure's interior and exterior sections that increase the drying shrinkage. A proper mix proportion of concrete should be maintained to improve the workability and maintain a higher compressive strength after concrete hardening.

Moreover, concrete curing is the process of placing the concrete with sufficient moisture to ensure the concrete gains enough strength to delay drying shrinkage. Inadequate curing of concrete will increase shrinkage at the time when the concrete is at low strength, which leads to a decrease of compressive strength. Consolidation is a necessary process as placing the concrete will entrap air voids and form honeycomb concrete after hardening. Insufficient consolidation and incorrect concrete placement will result in concrete cracks from its load before it has developed enough strength to support itself. Other than poor construction practice, the formation of concrete cracks may also occur

due to errors in the design phase, chemical reactions, and corrosion of reinforcement.

2.3 Destructive Testing

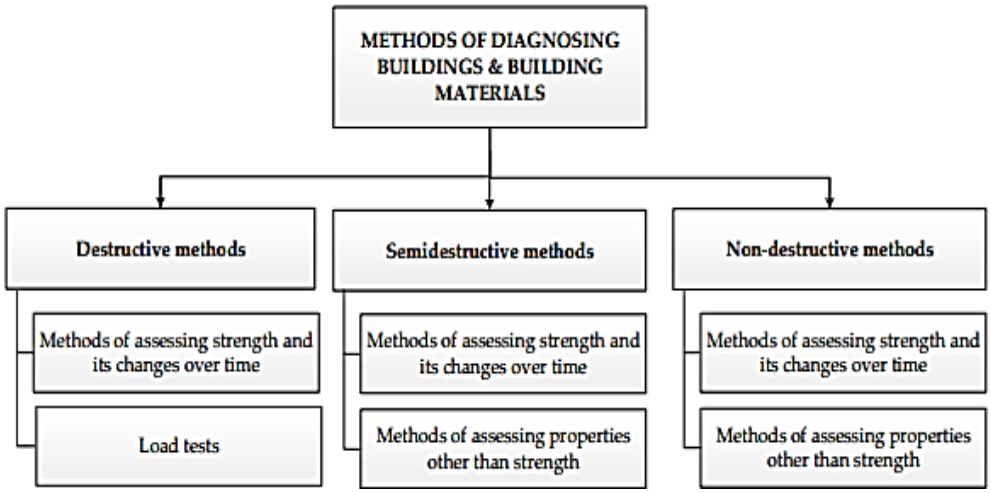

Figure 2.1: The general classification of investigation methods that is suitable for diagnosing buildings and building material (Schabowicz, 2019).

As shown in Figure 2.1, there are 3 methods in diagnosing buildings and building material, namely the destructive test (DT), semi destructive test (SDT) non-destructive test (NDT). Destructive testing (DT) is a test that carried out to determine the mechanical properties of concrete. The term destructive refers to the test, which includes the crushing of concrete to obtain concrete strength. DT is suitable to be adopted when the amount of concrete mix is produced on a large scale. It is relatively easy testing to be carried out and can yield accurate results for interpretation. It is also a cheaper approach in comparison to NDT in terms of equipment cost. The concrete cube test, splitting tensile strength test, and flexural strength test are examples of DT. For DT, the concrete strength test will be carried out to test the results for 7 days, 14 days, and 28 days; some tests might cost up to 90 days for a more accurate study. There are a few disadvantages of DT as the concrete specimens used in this testing will be destroyed and cannot be reused. DT is also not applicable to the early stage (before 7 days) of the concrete hardening process.

2.4 Non- Destructive Testing

Non-destructive testing (NDT) is also commonly known as non-destructive evaluation (NDE). NDT is an approach used to inspect the material without destruction and not affect its future use (Chakraborty et al., 2019). NDT is used to test the properties of various materials, for example, concrete, wood, steel, and mansory. NDT is usually carried out during the service life to examine the strength, detect cracking, check for corrosion of the reinforcement bar and void in the concrete. It is frequently used in new structures as it can examine the integrity of the structure and, at the same time, without damaging it. Ultrasonic Testing (UT), Thermography Method, and Magnetic Particle Testing (MT) are examples of NDT. NDT is widely used nowadays as it produces accurate results to allow repairation of the structure to prevent sudden failure. As shown in Figure 2.2 is the types of NDT can be used to examine the building structures and building materials. The main disadvantage of NDT is that the operation requires skilled workers, and the accuracy of the result will be limited if the concrete specimen is irregular.

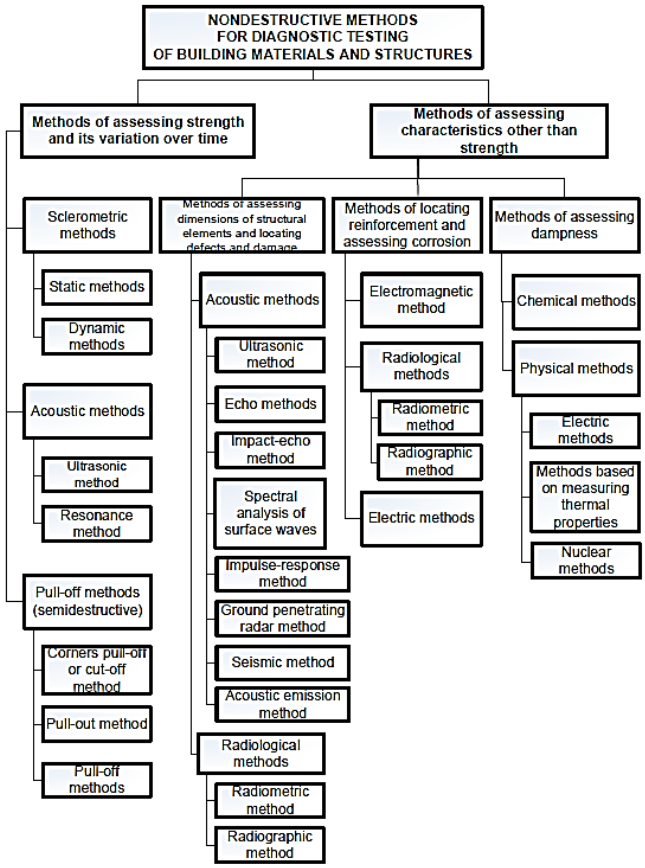

Figure 2.2: The types of non-destructive methods that is suitable for diagnosing building structures and building material (Schabowicz, 2019).

2.4.1 Ultrasonic Testing

Ultrasonic testing is a type of NDT, where the name ultrasonic testing comes from the word ultrasound. Ultrasound is a type of high-frequency acoustic wave which is approximately higher than 20kHz. Thus, it cannot be heard by humans. Therefore, the sound wave is used to detect the quality and defects in a material. The frequency used in ultrasonic testing will be based on the density of the material. A higher frequency (approximately 2 – 10 MHz) needs to be adopted to inspect metals and plastics, whereas a lower frequency (approximately 50 – 500 kHz) will be required to inspect concrete and wood. Wavelength is inversely proportional to the frequency. Therefore, when the wavelength increases, the frequency decreases. There are different types of ultrasonic testing, and the comparison of different techniques is shown in Table 2.1. Attenuation is known as the amplitude decrease due to energy loss when it travels through a medium. A sufficient frequency should be provided to examine a material to prevent the occurrence of attenuation. There are a few advantages of applying ultrasonic testing: -

- The high penetration of elastic wave is applicable in almost all sorts of material.
- It has high accuracy in detecting the location and measuring defects.
- Even a small defect can be detected using ultrasonic testing.

Table 2.1: Comparison of different ultrasonic testing (Yilmaz et al., 2020).

Techniques	Capabilities	Limitations
Immersion testing	MHz range operating frequency, coupling uniformity, less wear for probes, focused beams.	Limited materials due to corrosion.
Air-coupled testing	50 kHz to 2 MHz operating frequency, contactless coupling, focused beams.	High attenuation loss at higher frequencies, lower signal to noise ratio due to acoustical mismatch.
Contact Guided Wave (GW) testing	Up to 5 MHz operating frequency, the ability for faster inspection than air-coupled, superior coupling over immersion, and air-coupled methods hence higher transmissibility.	Wear of transducers and the material due to contact. Requires a special setup for angle excitation.
Air coupled excitation and contact reception Guided Wave (GW) testing	Possibility of mode selection, directional wavefront, long-range inspection.	Lower the signal to noise ratio.

2.4.1.1 Contact Ultrasonic Testing

Contact Ultrasonic Testing method refers to the transducer that will be placed directly on the concrete specimen. For the contact method, gel couplant is needed to be applied on the transducer before starting the test to ensure better contact between the concrete specimen and the transducer. The gel couplant applied can ensure that the wave propagates along with the concrete specimen without any air gaps (Ongpeng, Oreta, and Hirose, 2018). The presence of air gaps will cause the distortion and scattering of the wave. It will further affect the accuracy of the experimental results.

2.4.1.2 Non-contact Ultrasonic Testing

On the other hand, the non-contact ultrasonic test is also known as the air-coupled ultrasonic method. This method can effectively be carried out without considering the presence of air gaps and the usage of gel couplant. Gel couplant is not needed, as the transducer is not contacting the concrete specimen, air will act as the acoustic coupling medium. The non-contact ultrasonic test usually uses the air-coupled ultrasonic transducer to replace the conventional transducer. The air-coupled sensor was introduced in the 1970s, where it is generally used in wood inspection (Ongpeng, Oreta, and Hirose, 2018). Nowadays, this method is developed and widely used in the construction industry to analyze concrete quality. It is sensitive in detecting the defects in composite material and metals. For the non-contact method, a low frequency (lower than 100 kHz) is recommended to increase the sensitivity.

2.5 Parameters of Waves

Talking about waves, it involves the transportation of energy from one location to another. The energy is transported by the interaction between particles in a medium. During the transportation of energy, only energy will be transported but not the matter. The displacement of the particle will occur when a wave travels through a medium. After that, the particles will return to their original position (Physics Tutorial: What is a Wave?, 2020). The waves' travel speed depends on the density of the medium. For example, the wave's travel speed in the air is approximately 343 m/s, whereas, in a denser medium like water, the wave's travel speed is higher, which is approximately 1500 m/s. As shown in

Figure 2.3 is the wavelength, amplitude, and frequency of a wave. Wave travel from a crest to another crest indicates a full wave cycle. The time taken to complete one wave cycle is known as the period (T). Frequency is defined as the number of oscillations per second. Wavelength (λ) is the distance between the crest of a wave to another crest. It can be seen that wavelength is inversely proportional to the frequency. When the wavelength increases, the frequency decreases. Amplitude is known as the displacement of the particle from its original position. A greater amplitude indicates that the wave is carrying more energy.

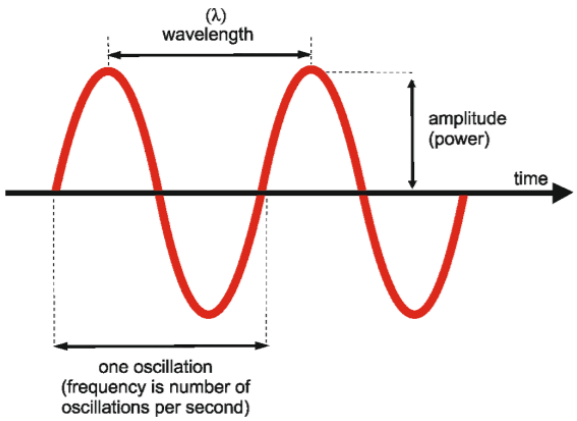

Figure 2.3: The wavelength, amplitude and frequency of a wave (Confuorto et al., 2016).

2.6 Types of Elastic waves

Elastic waves are also known as seismic waves with low amplitude, and the particle velocity is linearly proportional to the amplitude. When the wave's amplitude exceeds the elastic limit, the pulse will further decompose into an elastic wave and plastic wave. Elastic waves can be generated by human means such as using impact sources or occurs naturally, such as thunder. Wave speed is different from the speed of particles. The wave speed is the waves' travel speed through a medium, whereas particle speed is the movement of particles about their equilibrium position. Elastic waves can be further classified into body waves and surface waves. The classification of waves is based on the propagation direction of waves and the boundary condition. As shown in figure 2.4 is the classification of elastic waves. In terms of seismology, body waves can propagate into the earth's inner layer, whereas surface waves will only travel along the earth's surface. In terms of elastic wave theory, it can be said that

longitudinal waves have the maximum velocity, followed by the transverse, wave and the minimum velocity is the Rayleigh wave (Elastic Wave – an overview | ScienceDirect Topics, 2020).

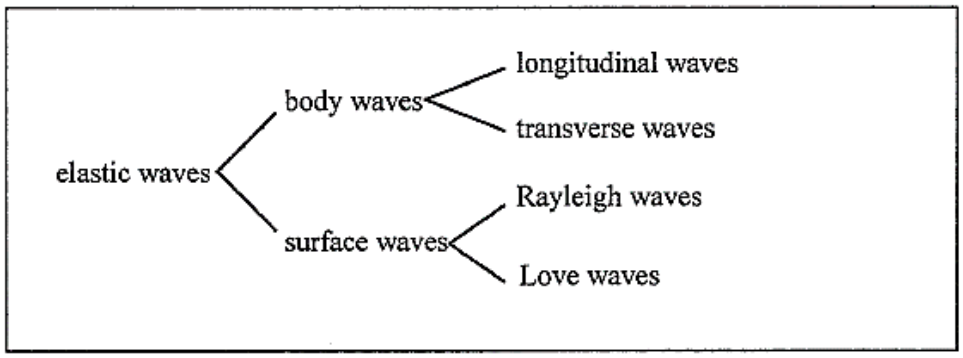

Figure 2.4: Principal types of progressive elastic waves (Novotny, 1999).

2.6.1 Body waves

Body waves can propagate into a medium. There are two common types of body waves, namely longitudinal waves and transverse waves. Body waves can propagate through an isotropic and a homogeneous medium. In terms of seismology, body waves can penetrate the earth's crust. Body waves have a higher frequency than surface waves. Thus the arrival of body waves will be earlier than surface waves (Endsley, 2007). When earthquakes occur, the longitudinal wave will first experience and be followed by the transverse wave.

2.6.1.1 Longitudinal waves

In terms of seismology, longitudinal waves are also known as primary waves (P- waves). A longitudinal wave moves fastest among the seismic wave. These waves do not rotate; it propagates through a medium by compression and rarefaction. The particle motion moves in the direction that is parallel to the wave travels. As shown in Figure 2.5, it can be noticed that the propagation of the wave and particle movement of the longitudinal wave moves in a horizontal direction. With the compression and rarefaction of wave movement, the compression zone and dilation zone will be formed along with the medium. Compression zone forms due to the particles are closely packed, whereas the dilation zone forms due to the particles being far apart. The primary wave's

typical velocity is 5 – 7 km/s in Earth's crust (mailto:www-bgs@bgs.ac.uk, 2020). Sound waves and ultrasound waves are examples of longitudinal waves.

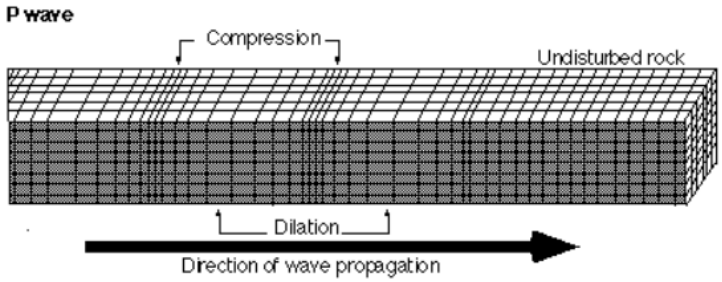

Figure 2.5: Propagation of P – wave (Bruce A.Bolt, Earthquakes: A Primer: W.H.Freeman & Company, 1978).

2.6.1.2 Transverse waves

In terms of seismology, transverse waves are also known as secondary waves (S-waves). In comparison, transverse waves move much slower than longitudinal waves. When a transverse wave propagates through a medium, shearing and rotation will be involved, but the volume will remain unchanged. As shown in Figure 2.6, it can be noticed that the propagation of the wave in a horizontal direction and particle movement moves in a perpendicular direction of the wave transfer. A transverse wave's typical velocity is 3 – 4 km/s in Earth's crust (mailto:www-bgs@bgs.ac.uk, 2020). Ripples on the water surface and electromagnetic waves such as microwaves and radio waves are examples of a transverse wave.

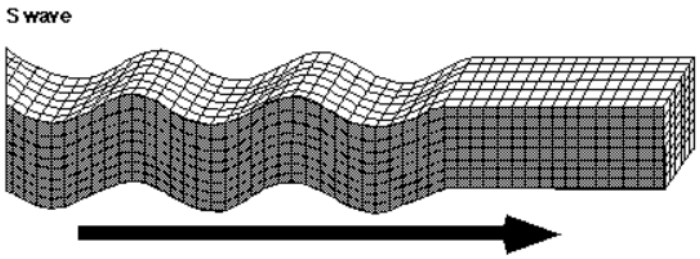

Figure 2.6: Propagation of S – wave (Bruce A.Bolt, Earthquakes: A Primer: W.H.Freeman & Company, 1978)

2.6.2 Surface waves

Surface waves can travel along the surface of a medium. There are two common types of surface waves, namely, the Rayleigh wave and the Love wave. Surface waves have a lower frequency than body waves, but they have a larger

amplitude than body waves. When earthquakes occur, surface waves are the one that causes damage and destruction. The typical velocity of surface waves is 2 – 4.5 km/s in typical Earth's crust (mailto:www-bgs@bgs.ac.uk, 2020).

2.6.2.1 Rayleigh waves

Rayleigh waves are named after John William Strutt, 3rd Baron Rayleigh discovered this wave in 1855. It is a type of surface acoustic wave which also known as R – wave. As shown in Figure 2.7 is the movement of the Rayleigh wave. The Rayleigh wave movement is in an elliptical motion, which causes the up and down movement. For example, the earthquake's shaking effect is caused by the Rayleigh wave (Eraky et al., 2018). The movement of the Rayleigh wave is similar to the movement of the ocean wave. The movement is approximately 10 % slower than the transverse wave. The Rayleigh wave is frequently used to detect a subsurface crack in concrete due to its sensitivity as it has high energy. The Rayleigh wave has a lower frequency in comparison to the body wave. Thus, it has a longer wavelength to provide deeper penetration. However, past studies show that the Rayleigh wave's penetration depth is limited to one wavelength depth.

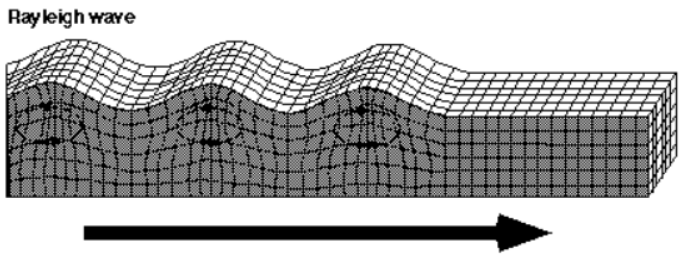

Figure 2.7: Propagation of Rayleigh wave (Bruce A.Bolt, Earthquakes: A Primer: W.H.Freeman & Company. 1978).

2.6.2.2 Love waves

Augustus Edward Hough Love is a British mathematician that discovers the mathematical model of this wave. Therefore, this type of wave is named after him. Love waves move faster than Rayleigh waves. As shown in Figure 2.8, the movement of love waves is almost the same as the transverse wave, but particles' movement is in a horizontal direction. The horizontal motion generated leads to horizontal shear and causes damage to the structure's foundation. The velocity of the Love wave is directly proportional to the frequency.

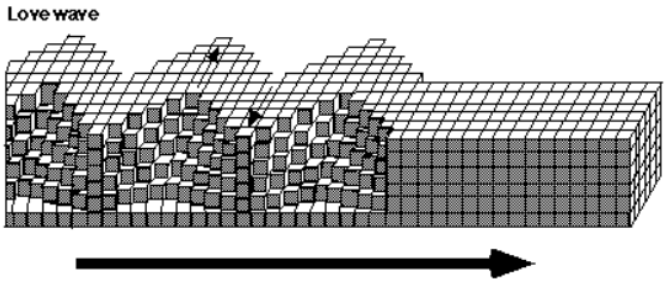

Figure 2.8: Propagation of Love wave (Bruce A.Bolt, Earthquakes: A Primer: W.H.Freeman & Company. 1978).

2.7 Past research study in subsurface crack analysis

The presence of subsurface cracks is relatively dangerous, which will lead to the sudden collapse of a structure. Thus, many research studies were conducted, and various experiments were conducted using different methods to resolve this issue. Some researchers had also proposed a new approach to improve the effectiveness in detecting a subsurface crack in the concrete.

2.7.1 FMC SAFT image

FMC SAFT image is known as the Full Matrix Capture Synthetic Aperture Focusing Technique. SAFT image is a type of ultrasonic inspection which utilizes the penetration of compressional wave or shear wave. The waveforms were collected with the aid of a transducer, pulse receiver, and oscilloscope. (Ghosh, Beniwal and Ganguli, 2015) compared the results between multiplicative FMC SAFT image and conventional additive FMC SAFT image. The results obtained were shown in Figure 2.9. It can be seen that the multiplicative FMC SAFT image has a more significant image in comparison with the additive FMC SAFT method. The SAFT image obtained can effectively illustrate the location of the subsurface cracks. Thus, it can be said that the multiplicative FMC SAFT image better visualized the location of the subsurface crack.

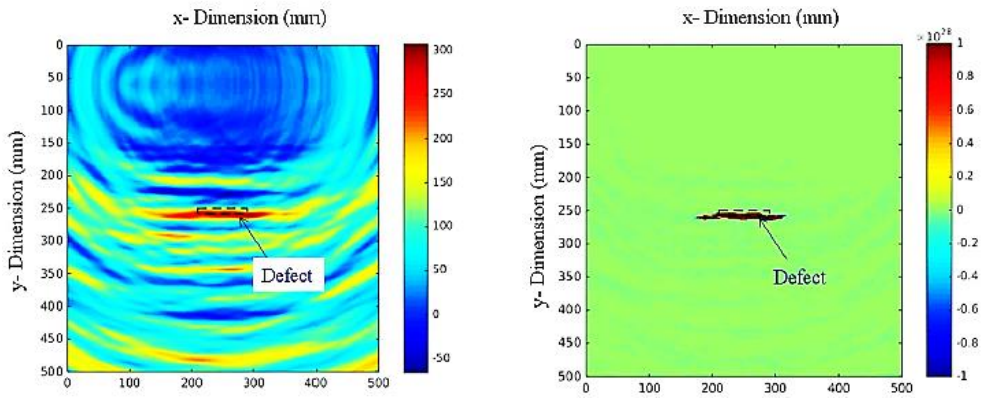

(a) (b)

Figure 2.9: Image with preprocessed signals using (a) Additive FMC SAFT image method (b) Multiplicative FMC SAFT image method (Ghosh, Beniwal and Ganguli, 2015).

2.7.2 Thermography

Thermography is a method that utilizes the infrared camera to produce a heat pattern image. Before the experiment starts, the concrete specimen needs to be heated in the oven at a temperature of 90 ℃ for 3 hours. (Aggelis et al., 2011) adopted the thermography approach to characterize the subsurface cracks in concrete. The results obtained were tabulated in Figure 2.10. It can be seen that a narrowing zone can be observed in the area of the crack. The thermograph obtained from a longer crack shows more significant results in comparison with the shorter crack.

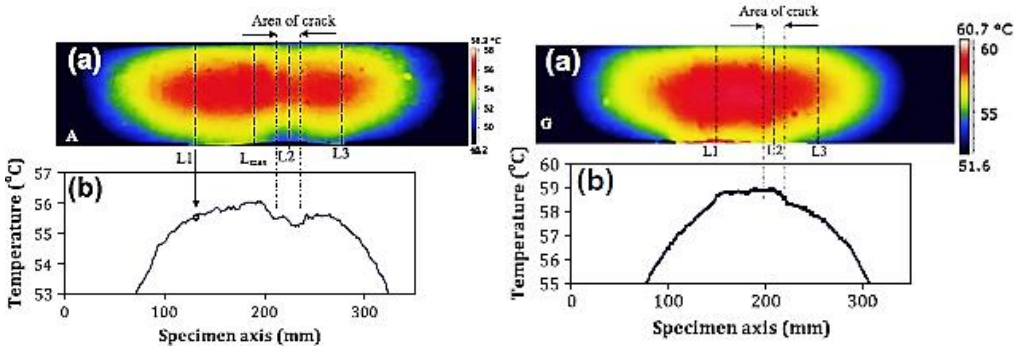

(a) (b)

Figure 2.10: The thermograph and average temperature of specimen with midspan deflection (a) 3 mm (b) 0.5 mm (Aggelis et al., 2011).

2.7.3 FDTD Simulations

FDTD is known as the Finite-Difference Time-Domain method, which is classified as a numerical analysis using approximate solutions. It solves Maxwell's equation, and a single simulation can cover a wide range of frequencies. (Ghosh et al., 2018) developed a two-dimensional strain-based FDTD model using software named MATLAB®. A vertical subsurface crack was simulated to determine the interaction between subsurface crack and Rayleigh wave. The results obtained were illustrated in Figure 2.11. It can be seen that the Rayleigh wave propagates along with the concrete, and it encounters the subsurface crack. After the Rayleigh wave interaction with the crack, part of the wave was reflected, and another part of the wave continues to propagate along its original travel direction.

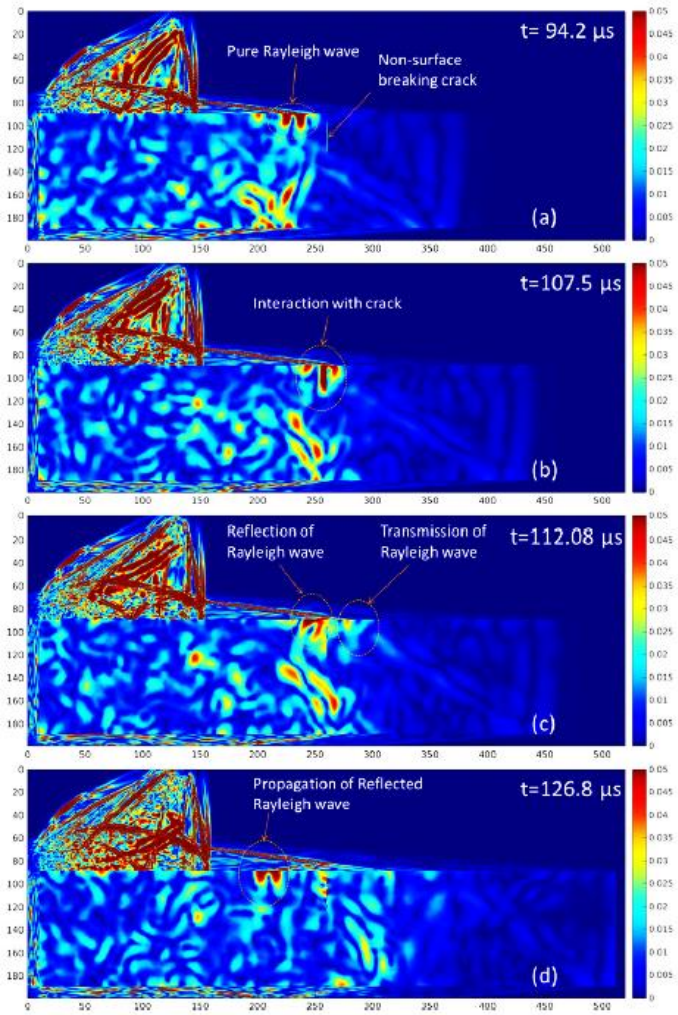

Figure 2.11: Interaction of R-wave with subsurface crack (a) Propagation of R-wave (b) Interaction of R-wave with subsurface crack (c) Reflection of R-wave (d) Propagation of reflected Rayleigh wave (Ghosh et al., 2018).

2.8 Summary of the Chapter

This chapter includes a literature review on the cracking in concrete, types of crack, and the poor practice in the construction industry that causes cracking in concrete. This chapter also discussed the methods used to diagnose building material, including the destructive test (DT) and non-destructive test (NDT). Ultrasonic Testing (UT) is a type of NDT that uses the propagation of sound waves to detect defects in the concrete. UT can be classified into contact-based ultrasonic testing and non-contact-based ultrasonic testing. The elastic wave types were also discussed in this chapter, which includes Longitudinal wave, Transverse wave, Rayleigh wave, and Love wave. Finally, some of the past research studies on the concrete subsurface cracks were also reviewed, which includes the FMC SAFT image, Thermography, and FDTD simulations.

CHAPTER 3

METHODOLOGY AND WORK PLAN

3.1 Introduction

This chapter presents the methodology and work plan adopted in this study. The experiment was carried out using the non-destructive test approach with the propagation of the Rayleigh wave. The experiment procedure involved raw material preparation such as cement, coarse aggregate, fine aggregate, water, and polystyrene board. Concrete specimens with an artificial subsurface crack were cast and tested using the non-contact method, and it was aid with a signal acquisition unit and a laptop. The waveform obtained was recorded and further analyzed using MATLAB®.

3.2 Flow Chart of the General Process

The general process of the experimental analysis was shown in Figure 3.1. Before the experiment was carried out, the literature review was done to understand, make comparisons, and determine the best method to conduct the experimental analysis. After the experiment was carried out, the results were obtained and further analyzed. Last but not least, a conclusion was made to summarize the experiment.

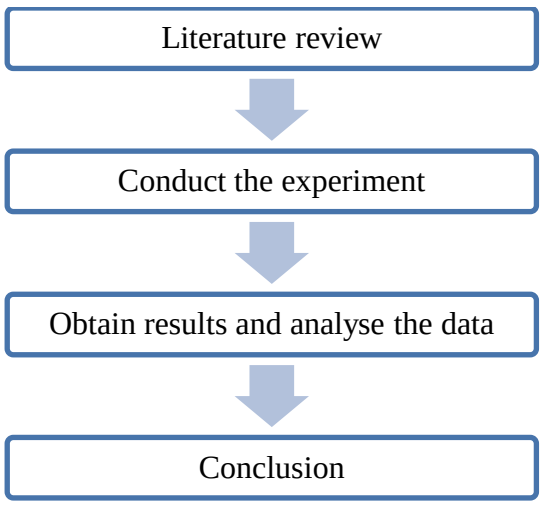

Figure 3.1: General process of the experimental analysis.

3.3 Experimental Analysis

The experimental method included preparing the correct amount of raw materials, placing artificial concrete subsurface crack, and casting concrete according to the proper mix proportion. After that, the sensors were placed at the proposed location, and frequencies were generated using different steel ball sizes followed by recording and analyzing the waveform. Lastly, the results were tabulated in the report, and discussions were made based on the results. The flow chart of the experimental analysis was tabulated in Figure 3.2.

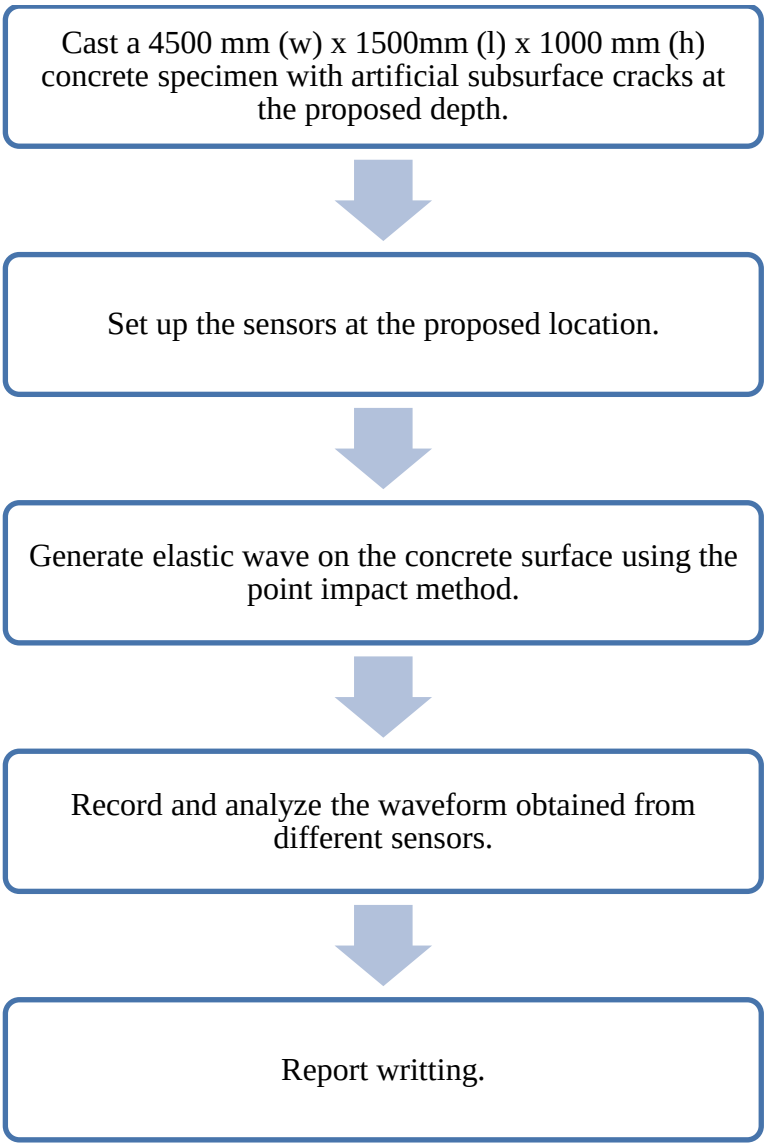

Figure 3.2: Flow chart of the experimental analysis.

3.4 Preparation of Raw Material

The cement, coarse aggregates, fine aggregates, and water were prepared in the desired mix proportions, as shown in Table 3.1. The concrete cast had a density of 2400 kg/m^3 with a concrete grade of G40. All of the raw materials were added and mix thoroughly until a homogeneous mix was obtained.

Table 3.1: Properties of concrete specimen.

Cement (kg/m^3)	**Water (kg/m^3)**	**Fine aggregates (kg/m^3)**	**Coarse aggregate (kg/m^3)**
3150	997	1750	1520

3.4.1 Cement

The usage of cement is a relatively crucial raw material in concrete casting. Under ASTM C150, the cement used for concrete casting in this research study is known as the Type 1 Ordinary Portland Cement. OPC is the most common cement used in the construction industry. It is a type of hydraulic cement that requires the presence of water for hardening and setting. When water is added, the cement acts as a binding agent to bind the aggregates and water to form concrete. The cement was sieved through the 300μm sieve and stored in an air-tight container to prevent moisture contact with the cement.

3.4.2 Coarse Aggregate

According to ASTM C33, aggregate with a size greater than 4.75 mm was determined as coarse aggregate. The aggregates come in all shapes and sizes. Both fine and coarse aggregates come together as mixed aggregates. Thus, sieve analysis was carried out to determine and separate coarse aggregate and fine aggregate from mixed aggregates. The sieve analysis was carried out, and the aggregates remain on the 4.75 mm, 10 mm, and 20 mm sieves were known as the coarse aggregate. The coarse aggregate used in the experimental analysis had a maximum size of 20 mm. The coarse aggregate obtained was put into the oven to dry for 24 hours at a temperature of approximately 100 ± 5 ℃ to ensure no moisture remains on the coarse aggregate.

3.4.3 Fine Aggregate

As mentioned above, sieve analysis was carried out to separate fine aggregates and coarse aggregates. Under ASTM C778, the aggregate ranges between 4.75 mm to 75μm were classified as fine aggregates. The sieve analysis was conducted, and the fine aggregate needed was collected. The fine aggregate was put into the oven to dry for 24 hours at a temperature of approximately 100 ± 5 ℃ to ensure no water remains on the fine aggregate, as it will affect the water-cement ratio of the fresh concrete.

3.4.4 Water

The water added is used to hydrate the cement and ensure the workability of the fresh concrete. In the mixing process of fresh concrete, the mixing water used should fit for drinking under ASTM C1602. The water should always free from contaminants and impurities. It is because the water's impurities will affect the concrete's properties and performance in long-term condition. In this research study, tap water was used as mixing water to produce concrete.

3.4.5 Polystyrene board

In this research study, the usage of polystyrene board is to act as the artificial subsurface crack. Polystyrene board was cut into the desired diameter (100 mm, 200 mm, 300 mm, 400 mm, and 500 mm) with a constant thickness of 5 mm. It was put into the mould to cast with the fresh concrete. Wire ties were used to tie the polystyrene board to ensure that the polystyrene board maintains at the proposed depth. The usage of polystyrene board as an artificial crack was because it has suitable acoustic impedance. The acoustic impedance is known as the ability of a wave to pass through a material. It is calculated by multiplying the density of material with the velocity of the wave. By comparing with concrete, the polystyrene board has a relatively low density. Thus, when the two materials' acoustic impendence has a significant difference, the wave will be reflected (Lee et al., 2019). Therefore, a polystyrene board has similar characteristics as a real subsurface crack, which can effectively act as an artificial subsurface crack.

3.5 Slump Test

The slump test was carried out to examine the consistency and workability of the fresh concrete. From the slump test result, one can determine whether the total amount of water added into the concrete mix was sufficient.

The fresh concrete was poured into the slump cone and in three equal layers. For every layer, a tamping rod is used to tap 25 times to ensure that the compaction of fresh concrete and the top layer was leveled using a trowel. After that, the cone was lifted slowly, and the concrete starts to slump. The original height of the cone was 300 mm. The change of height of the slumped concrete was called a slump. The change of height was measured, and it should always remain between 25 – 100 mm.

3.6 Casting of concrete

Before concrete casting started, a mould with a dimension of 4500 mm (L) x 1500 mm (W) x 1000 mm (H) was prepared with tightening bolts and nuts. The mould's inner surface should be cleaned and apply with a thin layer of oil before pouring the concrete mix into it. The oil applied is to ease the removal of mould after the hardening of concrete. In this research study, fresh concrete was cast together with a polystyrene board as an artificial crack. The polystyrene board was cut into the desired diameter and thickness. The artificial subsurface crack was set up at a depth of 25 mm, 225 mm, 425 mm, 625 mm, and 825 mm, as shown in Figure 3.3. The subsurface crack was set up at a spacing of 500 mm with a different diameter ranging from 100 mm to 500 mm, as shown in Figure 3.4. The concrete mix was placed into the mould together with the polystyrene board. A steel wire was used to tie the polystyrene board to ensure it stays at the proposed depth before the concrete hardens. Simultaneously, another 100 mm x 100 mm x 100 mm mould was prepared to cast a sample cube for the cube test.

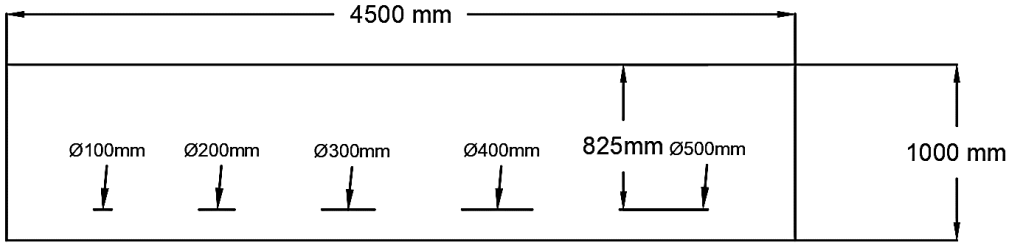

(a)

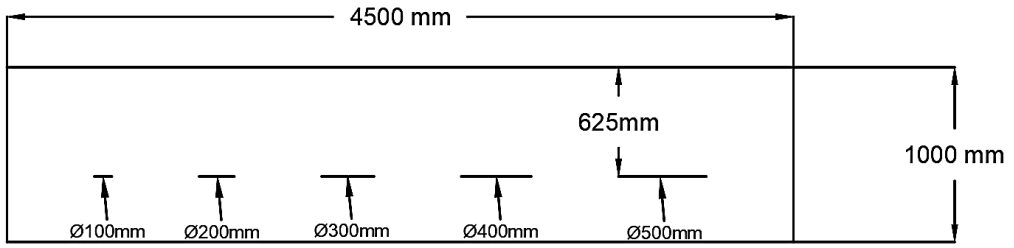

(b)

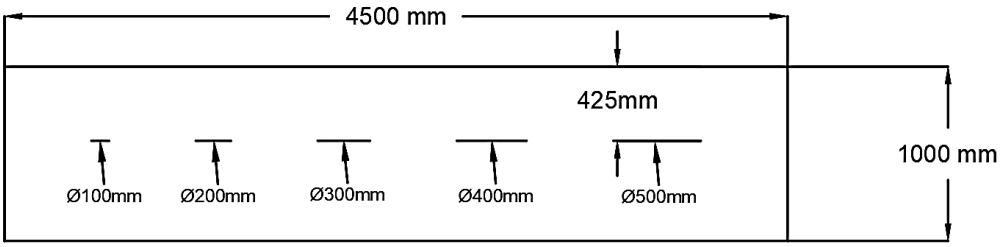

(c)

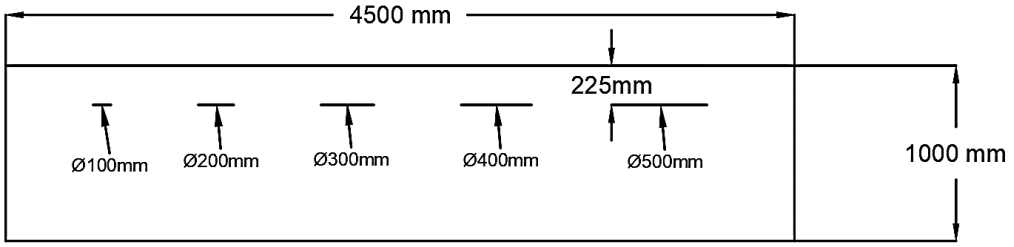

(d)

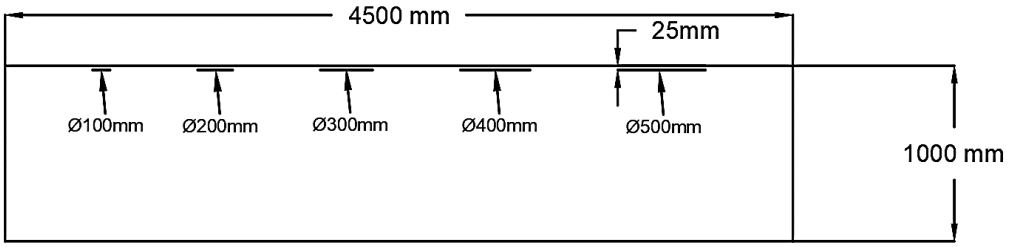

(e)

Figure 3.3: Side view of the concrete specimen with artificial subsurface crack set up at a depth of (a) 825 mm (b) 625 mm (c) 425 mm (d) 225 mm (e) 25 mm.

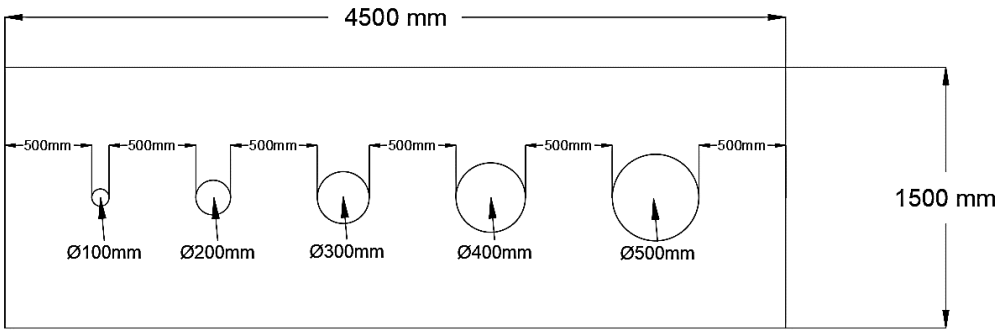

Figure 3.4: Plan view of the concrete specimen with artificial subsurface crack.

3.7 Curing of concrete

After pouring the concrete mix into the mould, it was left in an area to undergo a hardening process for 24 hours. After 24 hours, the concrete specimens were demoulded and underwent an air curing process. The process of concrete curing was maintained under proper moisture and temperature. Curing was done to prevent moisture loss from the concrete surface or maintain the concrete's mixing water during the hardening process. It is essential to help in the early age strength gaining of concrete. In this research study, the concrete specimens were cured for 28 days, and it is ready for subsurface crack detection.

3.8 Compression Strength Test

The compressive strength of concrete is known as the ability of the concrete specimen to withstand under compression. A compressive strength test was carried out for the curing age of 7 days and 28 days. It was expected that the concrete specimen would reach 65 % of strength on 7 days and 99 % of strength on 28 days.

The concrete specimens were removed on the 7 and 28 curing days. The concrete specimens were placed in the space between the bearing surface of the compression test machine. After that, an uniaxial compression load at the rate of 0.2 kN/s was then gradually applied until the concrete specimen fails. The maximum load was recorded for further calculation of the compressive strength. The compressive strength of the concrete specimen was calculated using Equation 3.1. The compression strength test's result of concrete specimen in 7 days and 28 days of curing age was tabulated in Table 3.2.

$$f = \frac{P}{A} \quad (3.1)$$

where f = Compressive strength, N/mm^2,

P = Maximum load, N,

A = Area of concrete specimen, mm^2.

Table 3.2: The results of compression strength test of concrete specimen for 7 days and 28 days of curing age.

Cube	Age (days)	Weight (kg)	Bulk hardened density (kg/m^3)	Maximum Load (kN)	Compressive strength (N/mm^2)
1	7	8.00	2370.37	983.63	43.72
	28	8.00	2370.37	1164.52	51.76
2	7	7.93	2349.63	926.53	41.18
	28	7.93	2349.63	1178.44	52.69
3	7	8.02	2376.30	1005.05	44.67
	28	8.02	2376.30	1234.95	54.89
4	7	8.11	2402.96	864.84	38.44
	28	8.11	2402.96	1145.69	50.92
5	7	7.98	2364.44	849.72	37.77
	28	7.98	2364.44	1136.52	50.51

3.9 Procedures of waveform collection

The detection of the subsurface crack was carried out using 4 non-contact sensors. It was set up at a distance of 5 mm away from the concrete's surface at the proposed location, as shown in Figure 3.5. The different diameters of steel balls (10 mm, 15 mm, 20 mm, and 25 mm) act as the input source to generate the elastic waves. It was hammered on the surface of the concrete specimen to generated different frequencies of elastic waves. When the steel ball collides with the surface of concrete, the potential energy was transformed into an elastic wave which causes the displacement of particles. Sufficient acoustic energy should be produced to prevent the happening of attenuation. The waveform collected by the sensors, further recorded by the signal acquisition unit, and the data were passed to the laptop. The setup of the apparatus was as shown in

Figure 3.5. After that, the data were further analyzed using the software called MATLAB®.

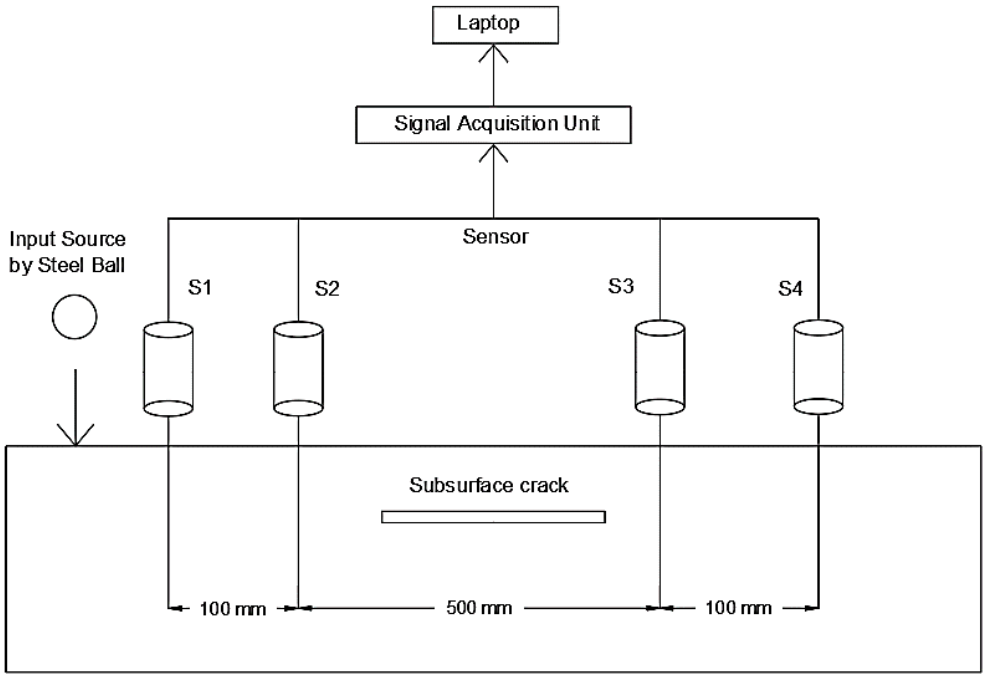

Figure 3.5: The set up of the apparatus.

3.10 Summary of the Chapter

All raw materials were prepared accordingly, and concrete specimens were cast according to the proposed depth and diameters of artificial subsurface crack. The concrete specimens were cured, and the compressive strength test was carried out. The experimental method involves detecting different diameters and depths of the artificial subsurface crack in the concrete specimen using different frequencies of elastic waves generated using a steel ball with different diameters. There was a total of 104 case studies conducted using this experimental method. The waveform results were collected by the 4 sensors placed at a location 5 mm above the concrete's surface. The elastic wave was generated, and the waveform results were collected and further analyzed using MATLAB®.

CHAPTER 4

RESULTS AND DISCUSSION

4.1 Introduction

This chapter illustrates and discusses the experimental results from the Rayleigh wave-based non-contact method. The discussions were made on the correlations of the Rayleigh wave's attenuation, propagation velocity, and dominant frequency when propagating through the concrete with different depths and diameters of subsurface crack. The waveform was collected and recorded by sensors that were connected to a signal acquisition unit. The waveforms obtained were further analyzed by using a software called MATLAB®.

4.2 Rayleigh wave

From the literature review, Rayleigh waves are surface wave which propagates in an elliptical motion on the surface which causes the up and down movement. Rayleigh wave can be easily differentiated from the longitudinal wave (P-wave) by the difference in propagation velocity of both waves, and it would increase with the travel distance. The Rayleigh wave's arrival time is characterized by a strong peak in the amplitude, which appears after the first arrival of the longitudinal wave (Lee, Lim, and Chai, 2015). As shown in Figure 4.1 was the maximum amplitude represented the waveform generated by a 15 mm diameter steel ball. The arrival of the Rayleigh wave was after the first arrival of the longitudinal wave.

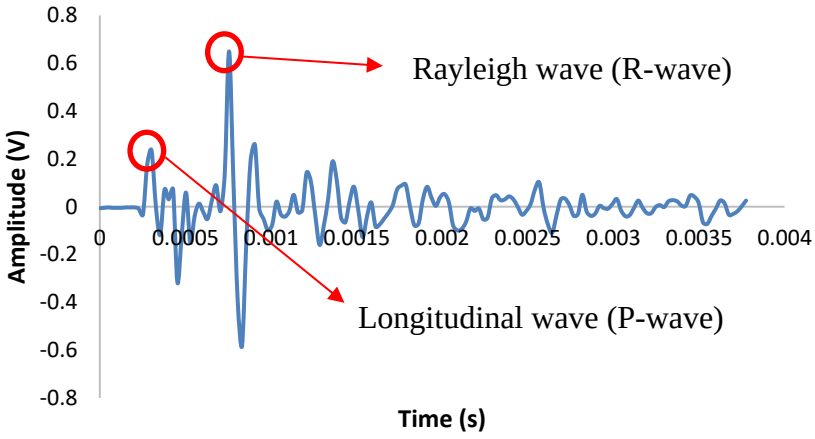

Figure 4.1: The waveforms received by sensor 1.

4.3 The excitation frequency

The concrete specimens with artificial subsurface crack were prepared for the experimental analysis. The elastic waves were generated by the steel ball hammers, which impacts the concrete surface. Different diameters of steel balls were used to generate different frequencies of Rayleigh waves in this research study. The Rayleigh waves were generated by the mechanical impacts of different diameters of steel balls (10 mm, 15 mm, 20 mm, and 25 mm) on the concrete specimen's surface. The mechanical impact caused the collision of particles between the steel ball with the concrete surface, and Rayleigh waves with different dominant frequencies were generated. The waveforms were received and recorded by the sensors set at 5 mm away from the concrete surface. From Table 4.1, it can be noticed that when the steel ball diameter increases, the frequency generated decreases. The wavelength is inversely proportional to the frequency. Therefore, when the frequency decreases, the wavelength increases, which indicates that a bigger diameter of steel ball produces an elastic wave with a longer wavelength.

Table 4.1: The Rayleigh wave's frequency generated using different diameters of steel ball.

Steel ball diameter (mm)	Frequency generated (kHz)
10	14.32
15	10.53
20	7.58
25	5.47

4.4 Time-domain analysis

For a time-domain graph, the amplitude fluctuates over time. Therefore, a time-domain graph shows how amplitude changes with time. In this research study, the waveforms were received and recorded by the sensors, and the waveforms were further processed using MATLAB®.

4.4.1 Time-domain analysis of Rayleigh wave

Figure 4.2 shows the time-domain graph of a sound concrete obtained from a 10 mm and 25 mm steel ball diameter. Figure 4.3 – 4.5 shows the time domain graph obtained from the experimental analysis for concrete with a subsurface crack at different depths of 25 mm, 425 mm, and 825 mm obtain from 10 mm and 25 mm diameter of steel ball, respectively. By comparing the time-domain graph in Figure 4.2 (a) and Figure 4.2 (b), one can notice that when the steel ball's diameter used to generate the elastic waves increases, the wave's amplitude increases. It would result in an easier determination of the arrival of the Rayleigh wave. The increase of steel ball diameter indicates the decrease in the frequency generated, as tabulated in Table 4.1. The finding shows that the amplitude is inversely proportional to the frequency.

By comparing the time-domain graph of the sound concrete and concrete with a subsurface crack, a significant delay of the Rayleigh peak between sensor 2 and sensor 3 was observed when there was a presence of a subsurface crack. The delay of the Rayleigh peak increases when the crack diameter increases. This phenomenon was most likely influence by the presence of artificial subsurface crack, which caused the elastic wave's scattering effect. Thus, when the crack diameter increases, the more evident the scattering effect.

The decrease in the amplitude of the Rayleigh peak was also noticed when the subsurface cracks depth increase. The Rayleigh wave's penetration depth is approximately one wavelength depth (Aggelis et al., 2011). The decrease in the Rayleigh peak amplitude most probably due to the limitation of depth penetration of the Rayleigh wave. A similar trend of the time-domain graph was obtained for the sound concrete and concrete with a subsurface crack at depths of 225 mm and 625 mm.

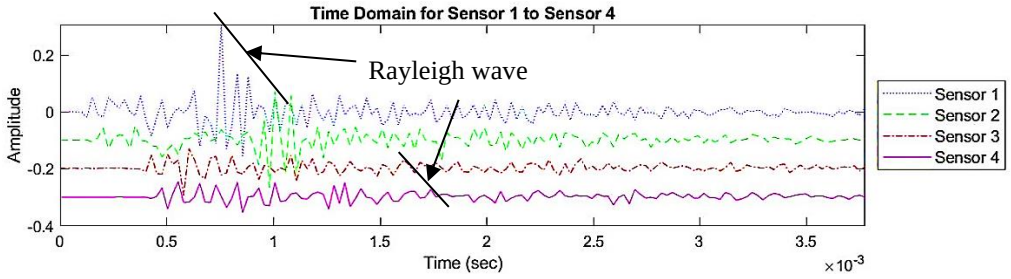

(a)

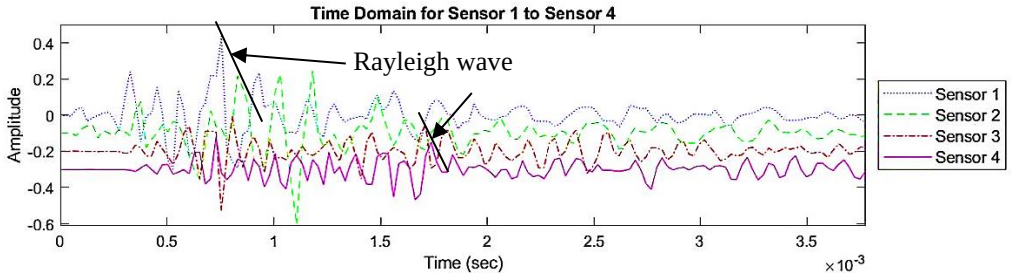

(b)

Figure 4.2: The time-domain graph of sound concrete obtained from (a) 10 mm diameter steel ball (b) 25 mm diameter steel ball.

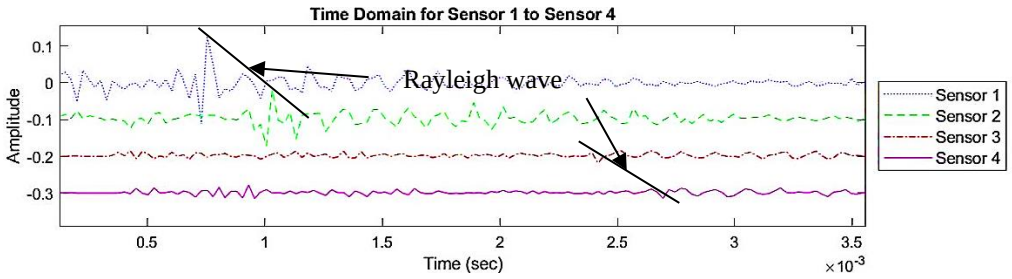

(a)

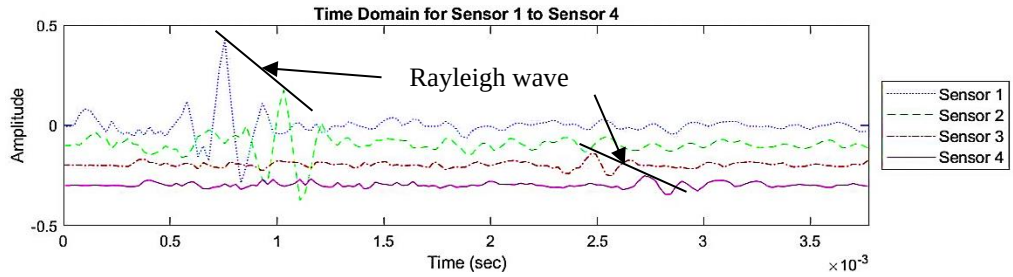

(b)

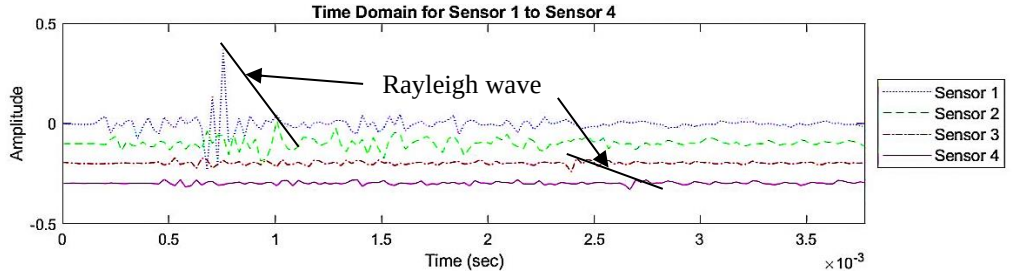

(c)

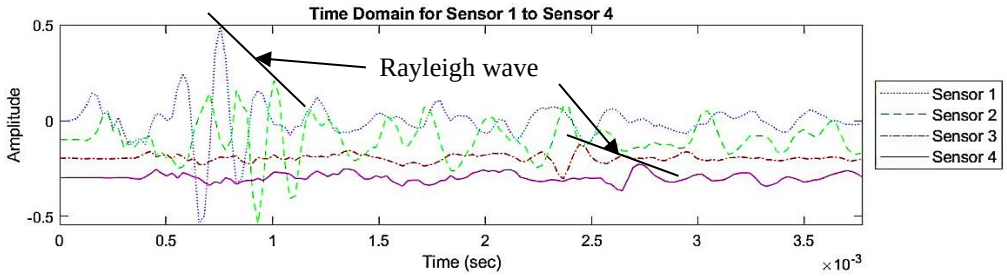

(d)

Figure 4.3: The time-domain graph of concrete with a subsurface crack at a depth of 25 mm (a) with 100 mm crack length obtain from 10 mm diameter steel ball (b) with 100 mm crack length obtain from 25 mm diameter steel ball (c) with 500 mm crack length obtain from 10 mm diameter steel ball (d) with 500 mm crack length obtain from 25 mm diameter steel ball.

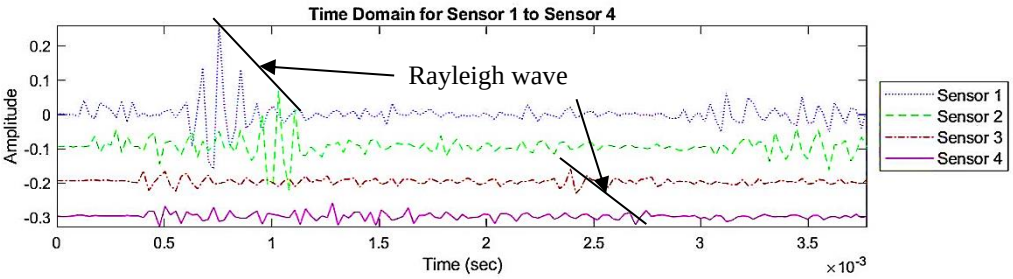

(a)

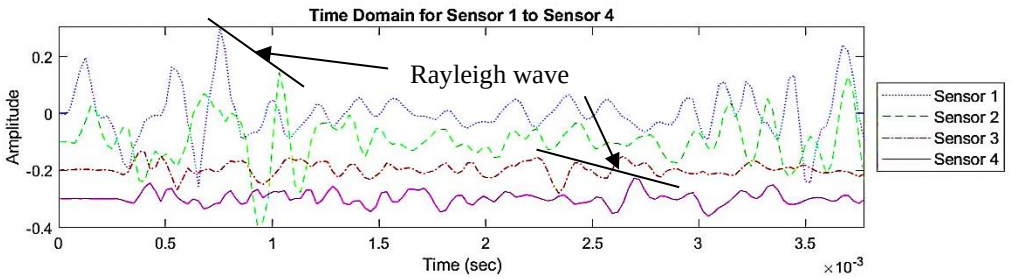

(b)

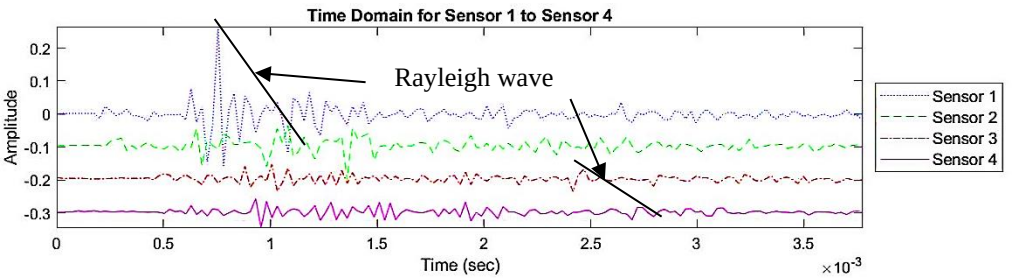

(c)

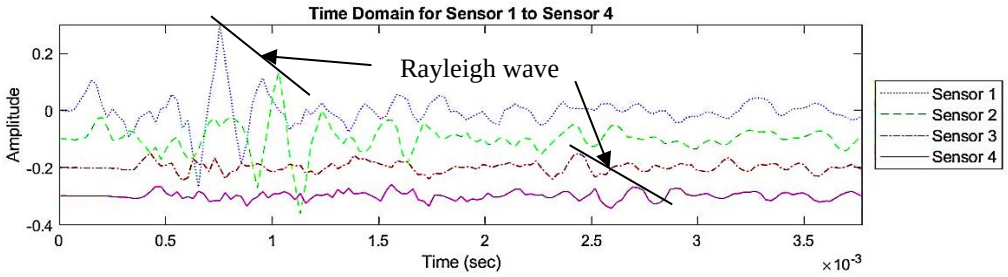

(d)

Figure 4.4: The time-domain graph of concrete with a subsurface crack at a depth of 425 mm (a) with 100 mm crack length obtain from 10 mm diameter steel ball (b) with 100 mm crack length obtain from 25 mm diameter steel ball (c) with 500 mm crack length obtain from 10 mm diameter steel ball (d) with 500 mm crack length obtain from 25 mm diameter steel ball.

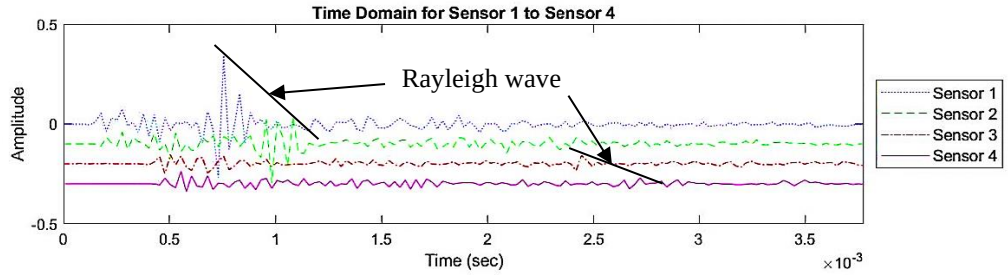

(a)

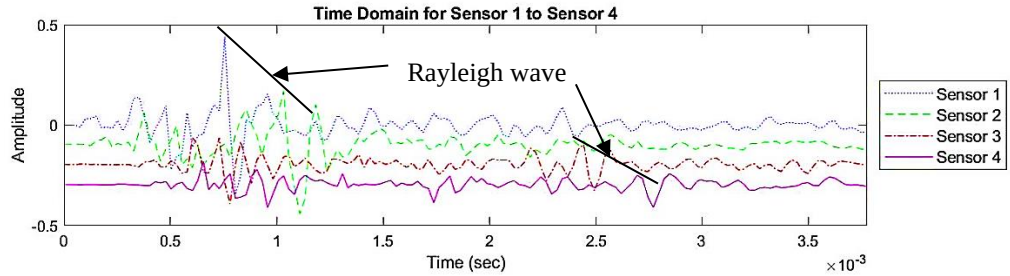

(b)

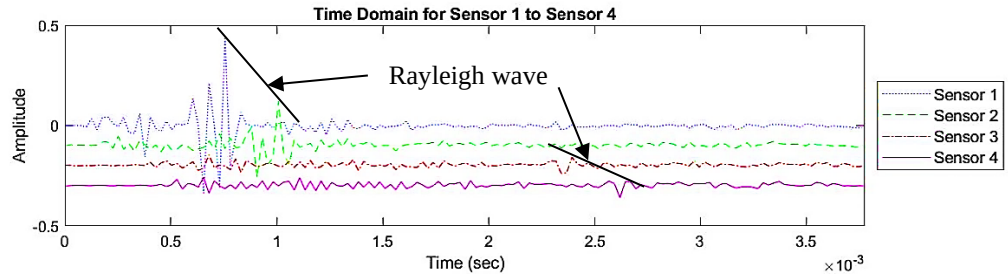

(c)

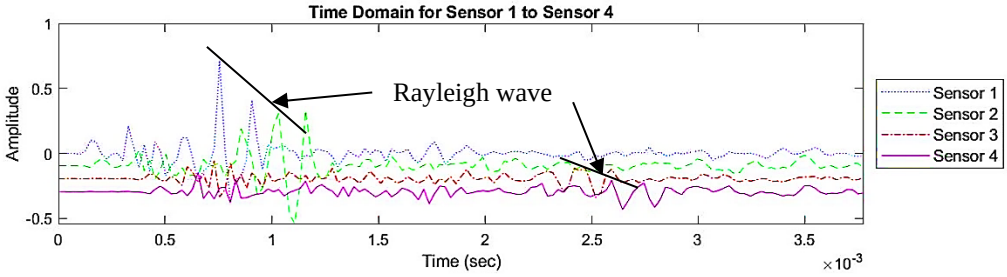

(d)

Figure 4.5: The time-domain graph of concrete with a subsurface crack at a depth of 825 mm (a) with 100 mm crack length obtain from 10 mm diameter steel ball (b) with 100 mm crack length obtain from 25 mm diameter steel ball (c) with 500 mm crack length obtain from 10 mm diameter steel ball (d) with 500 mm crack length obtain from 25 mm diameter steel ball.

4.5 Attenuation

Attenuation is known as amplitude decay when it propagates through the concrete specimens. Attenuation is caused by the combined effect of absorption and scattering of elastic waves. The process of elastic wave energy converted to other forms of energy is known as elastic waves' absorption. In contrast, the process of scattering happens when the elastic waves are reflected in directions other than their original propagation path (Attenuation of Sound Waves, 2019).

4.5.1 Attenuation rate

The decay of amplitude can be extracted from the time domain graph. The percentage of the Rayleigh wave's attenuation can be calculated by dividing the amplitude difference between the first sensor and the subsequent sensor by the amplitude of the first sensor, as shown in Equation 4.1.

$$A(\%) = \frac{A_{x+1} - A_x}{A_x}, when\ x = 1, 2, 3 \quad (4.1)$$

where $A(\%)$ = Percentage of attenuation,

A_x = Amplitude of the first sensor,

A_{x+1} = Amplitude of the subsequent sensor,

4.5.2 Attenuation rate of the Rayleigh wave

From the previous studies, (Aggelis, Leonidou, and Matikas, 2012) found out that amplitude is a sensitive parameter in determining the presence of a subsurface crack. The decay in amplitude can be observed, which is approximately 80 % compared to the sound concrete. The frequency of the wave is proportional to the percentage of attenuation. When the Rayleigh wave frequency increases, the percentage of attenuation increases (In et al., 2009)

Figure 4.6 – 4.8 represents the percentage of attenuation for the concrete subsurface crack at a depth of 25 mm, 425 mm, 825 mm obtain from 10 mm, 15 mm, 20 mm, and 25 mm diameters of steel ball, respectively. From the results obtained, it can be seen that the amplitude of the Rayleigh wave enormously decreases when the Rayleigh wave travels through the subsurface crack zone. Taking the case of a concrete specimen with a subsurface crack of 100 mm diameter at a depth of 25 mm obtained from 10 mm diameter of steel ball, the percentage of attenuation between sensor 1 and sensor 2 is 33.77 %, after that, a sharp increase in the percentage of attenuation of 88.31 % was observed between sensor 2 and sensor 3, the percentage of attenuation was then slightly increased to 90.91 % between sensor 3 and sensor 4. A similar increasing trend in the percentage of attenuation between sensor 2 and sensor 3 was also noticed from the concrete specimen with a subsurface crack at a depth of 225 mm and 625 mm.

The attenuation occurs due to the inhomogeneity of the polystyrene board and the concrete. The inhomogeneity of polystyrene board causes the scattering and geometrical spreading of the elastic wave, which causes the decay in amplitude. A high percentage of attenuation can be observed between sensor 2 and sensor 3 because the artificial subsurface crack was located between the sensor. Therefore, the subsurface crack location can be easily determined by observing the percentage of attenuation between sensors.

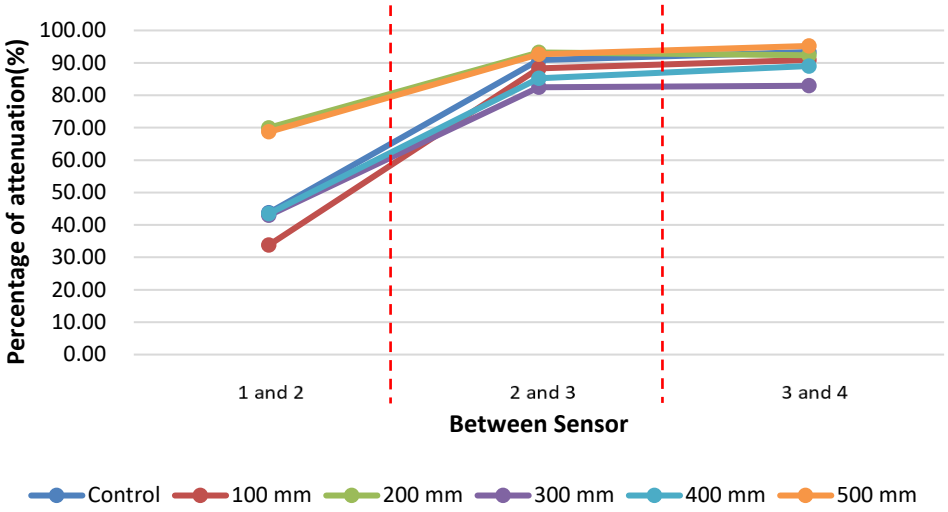
100.00
90.00
80.00
70.00
60.00
50.00
40.00
30.00
20.00
10.00
0.00
Percentage of attenuation(%)
1 and 2
2 and 3
3 and 4
Between Sensor
Control
100 mm
200 mm
300 mm
400 mm
500 mm

(a)

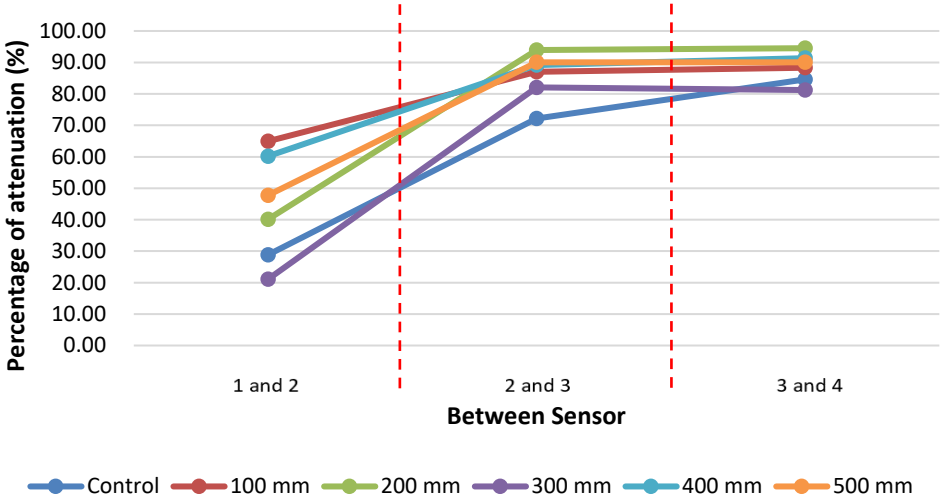
100.00
90.00
80.00
70.00
60.00
50.00
40.00
30.00
20.00
10.00
0.00
Percentage of attenuation (%)
1 and 2
2 and 3
3 and 4
Between Sensor
Control
100 mm
200 mm
300 mm
400 mm
500 mm

(b)

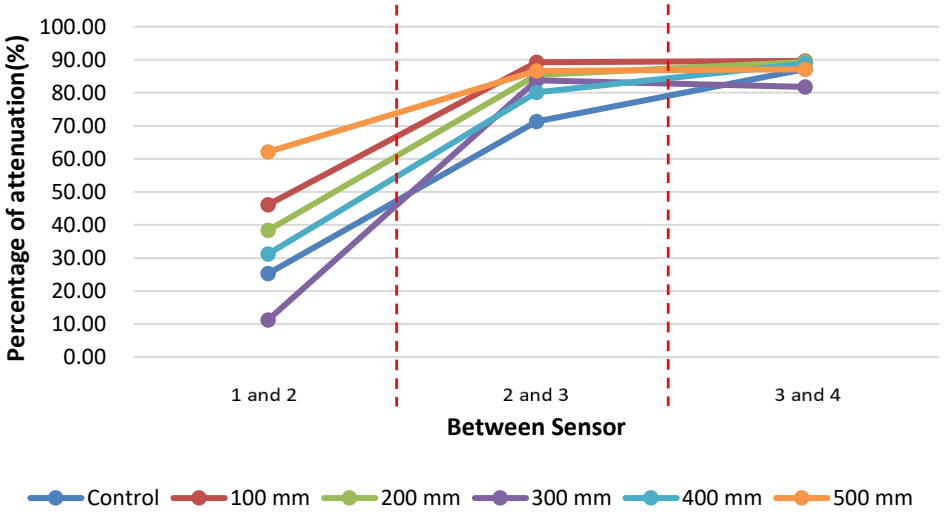
100.00
90.00
80.00
70.00
60.00
50.00
40.00
30.00
20.00
10.00
0.00
Percentage of attenuation(%)
1 and 2
2 and 3
3 and 4
Between Sensor
Control
100 mm
200 mm
300 mm
400 mm
500 mm

(c)

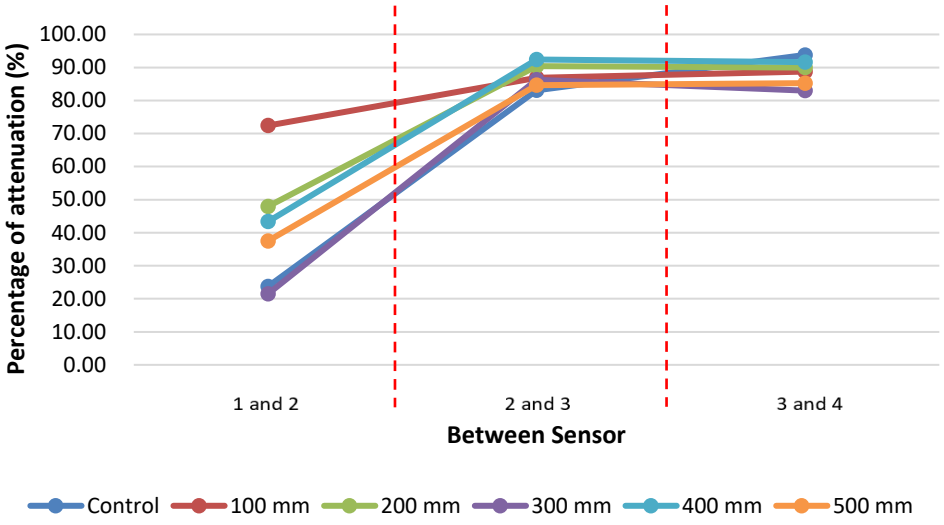

(d)

Figure 4.6: The percentage of attenuation for concrete with a subsurface crack at a depth of 25 mm obtained from (a) 10 mm diameter steel ball (b) 15 mm diameter steel ball (c) 20 mm diameter steel ball (d) 25 mm diameter steel ball.

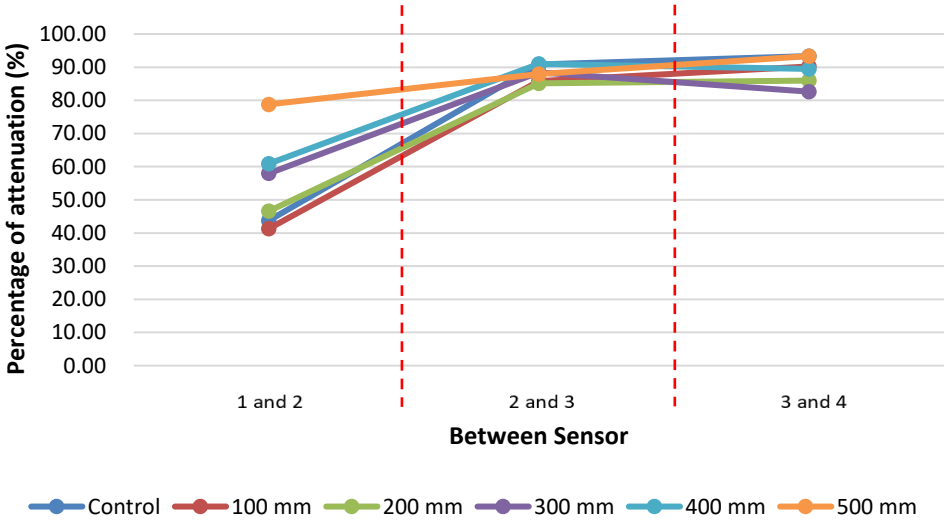

(a)

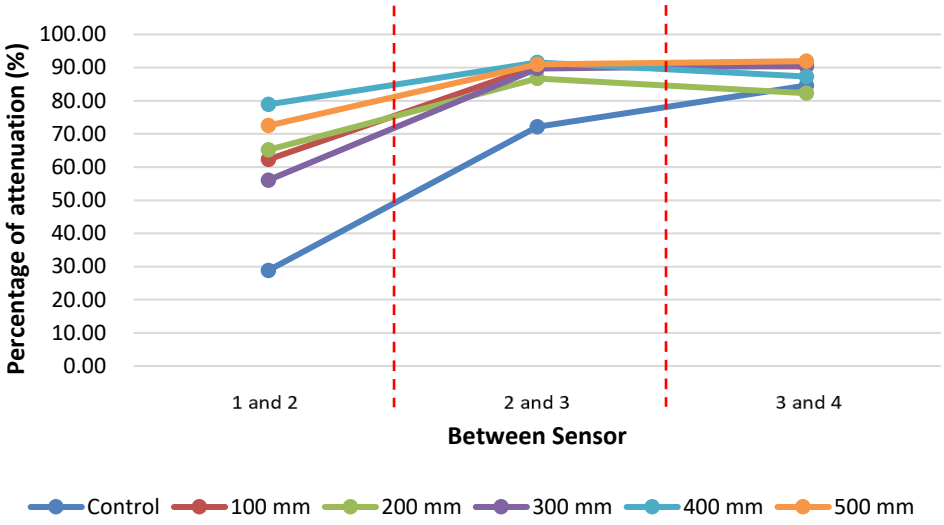
100.00
90.00
80.00
70.00
60.00
50.00
40.00
30.00
20.00
10.00
0.00
Percentage of attenuation (%)
1 and 2
2 and 3
3 and 4
Between Sensor
Control
100 mm
200 mm
300 mm
400 mm
500 mm

(b)

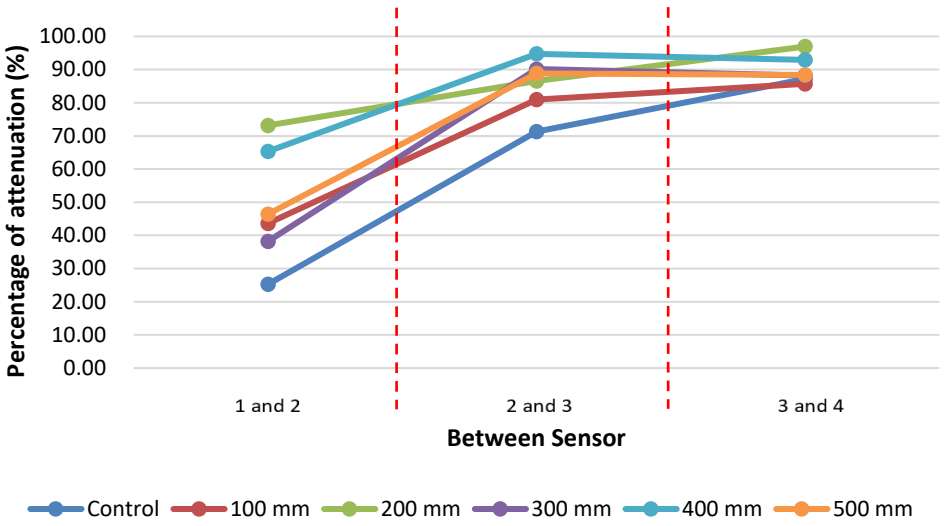
100.00
90.00
80.00
70.00
60.00
50.00
40.00
30.00
20.00
10.00
0.00
Percentage of attenuation (%)
1 and 2
2 and 3
3 and 4
Between Sensor
Control
100 mm
200 mm
300 mm
400 mm
500 mm

(c)

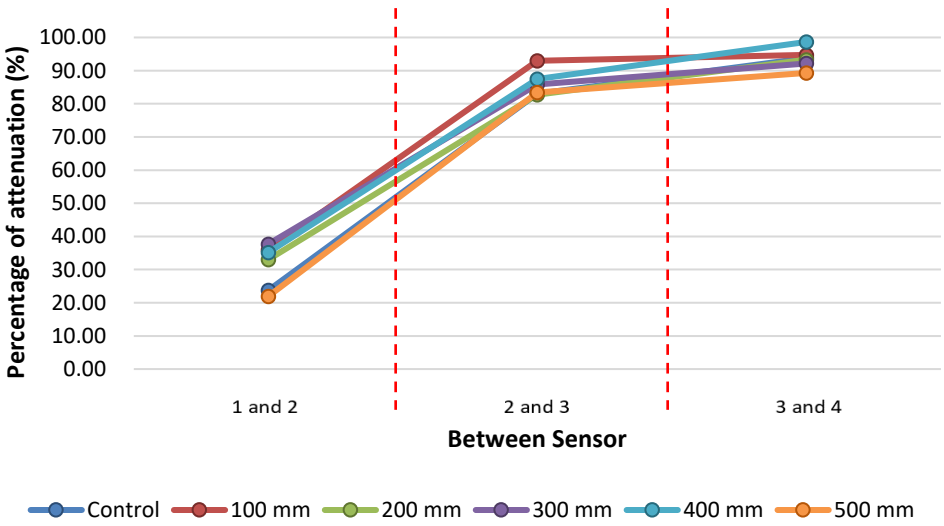
100.00
90.00
80.00
70.00
60.00
50.00
40.00
30.00
20.00
10.00
0.00
Percentage of attenuation (%)
1 and 2
2 and 3
3 and 4
Between Sensor
Control
100 mm
200 mm
300 mm
400 mm
500 mm

(d)

Figure 4.7: The percentage of attenuation for concrete with a subsurface crack at a depth of 425 mm obtained from (a) 10 mm diameter steel ball (b) 15 mm diameter steel ball (c) 20 mm diameter steel ball (d) 25 mm diameter steel ball.

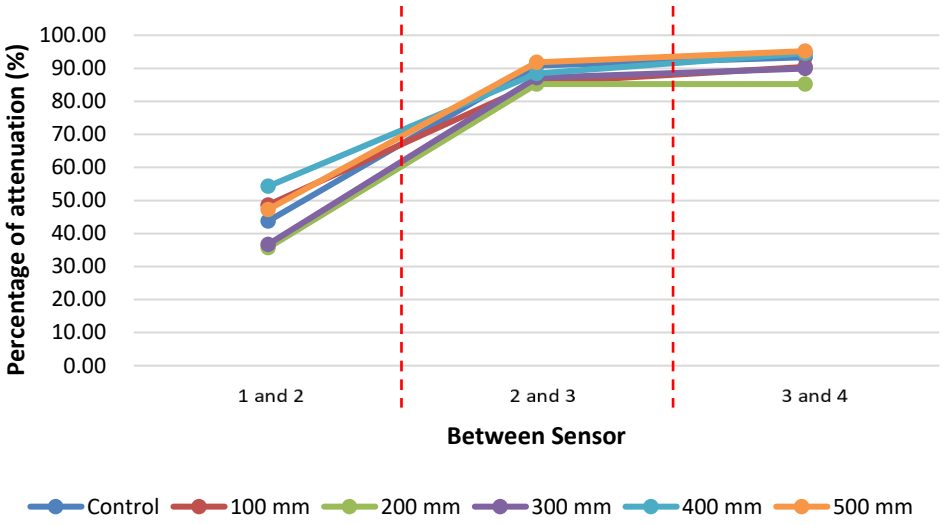

(a)

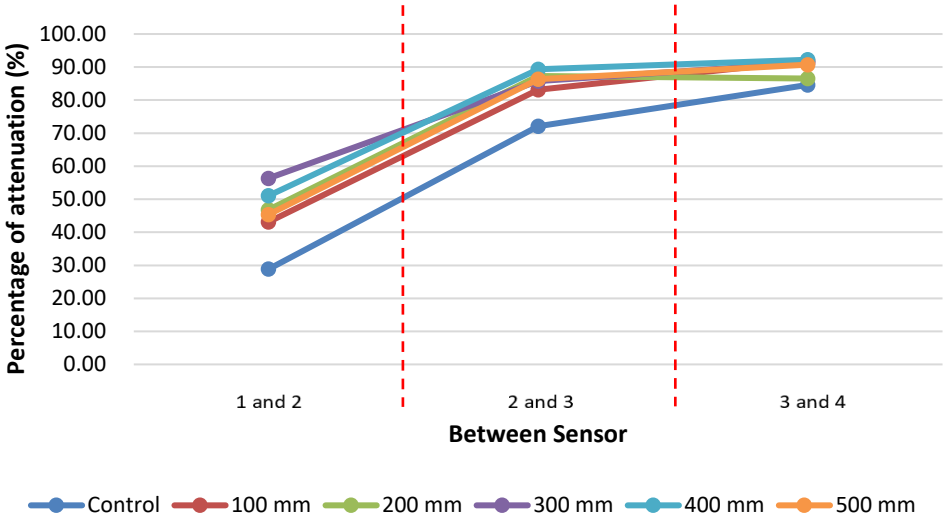

(b)

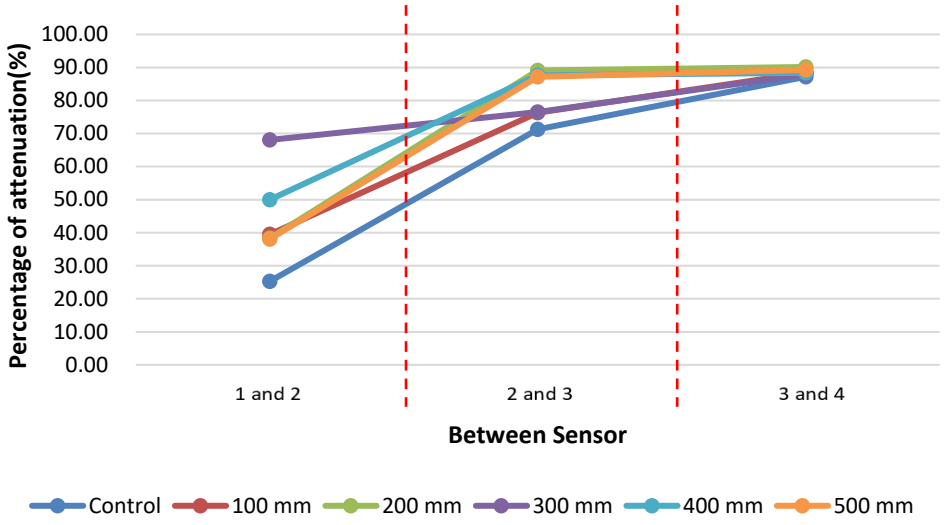

(c)

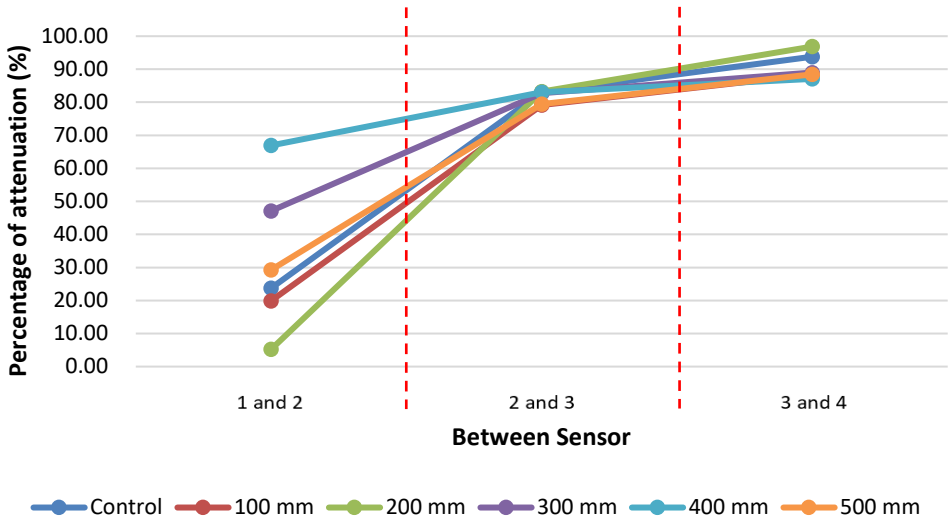

(d)

Figure 4.8: The percentage of attenuation for concrete with a subsurface crack at a depth of 825 mm obtained from (a) 10 mm diameter steel ball (b) 15 mm diameter steel ball (c) 20 mm diameter steel ball (d) 25 mm diameter steel ball.

The average percentage of attenuation for concrete with a subsurface crack at a depth varying from 25 mm to 825 mm obtain from steel balls of 10 mm, 15 mm, 20 mm, and 25 mm was tabulated in Table 4.2. The average percentage of attenuation between sensor 1 and sensor 2, between sensor 2 and sensor 3, and between sensor 3 and sensor 4 obtained from a 10 mm diameter of steel ball was 54.16 %, 87.69 %, 89.72 %, respectively. In contrast, the average percentage of attenuation between sensor 1 and sensor 2, between

sensor 2 and sensor 3, and between sensor 3 and sensor 4 obtained from a 25 mm diameter of steel ball were 34.91 %, 85.11 %, and 90.45 %, respectively. By comparing the average percentage of attenuation obtain from the steel ball with 10 mm and 25 mm diameter, it can be noticed that the percentage of attenuation for the 10 mm steel ball was higher in comparison with the 25 mm steel ball. When the diameter of the steel ball decreases, the frequency of the Rayleigh wave increases. It implies that a result with higher accuracy can be expected from a higher excitation frequency of the Rayleigh wave as the percentage of attenuation increases with the Rayleigh wave's frequency.

Table 4.2: The average percentage of attenuation for the concrete with a subsurface crack at different depth of delamination obtained from the different diameter of steel ball.

Steel Ball Diameter (mm)	**Depth of Delamination (mm)**	**Percentage of attenuation through each sensor (%)**		
		Between sensor 1 to sensor 2	**Between sensor 2 to sensor 3**	**Between sensor 3 to sensor 4**
10	25	51.77	88.36	90.08
	225	54.82	87.88	89.23
	425	57.11	87.64	88.32
	625	62.67	86.94	89.90
	825	44.51	87.63	91.07
Average		54.16	87.69	89.72
15	25	46.82	88.44	89.08
	225	32.97	83.72	89.07
	425	66.99	89.87	88.51
	625	43.22	87.36	89.72
	825	48.54	86.37	90.52
Average		47.71	87.15	89.34
20	25	37.82	85.04	87.35
	225	56.41	88.31	91.45

	425	53.37	88.26	90.45
	625	32.59	79.59	88.94
	825	46.79	83.36	88.83
Average		45.40	84.91	89.40
25	25	44.54	88.12	87.71
	225	26.48	85.28	91.01
	425	32.75	86.51	93.63
	625	37.07	84.10	89.96
	825	33.69	81.53	89.96
Average		34.91	85.11	90.45

Additionally, Figure 4.9 shows the average percentage of attenuation for concrete with a subsurface crack at different depths ranging from 25 mm to 825 mm. According to the graph, it can be seen that the average percentage of attenuation between sensor 2 and sensor 3 for concrete with a subsurface crack at a depth of 25 mm is 87.50 %. In contrast, the concrete with a subsurface crack at a depth of 825 mm had an average percentage of 84.70 %. The average percentage of attenuation decreases as the subsurface crack depth increases. Thus, one can say that the subsurface crack, which is nearer to the concrete surface, is more easily to be determined. These findings are probably because of the characteristics of the Rayleigh wave's penetration depth, which makes it not sensitive when the depth is over one wavelength depth.

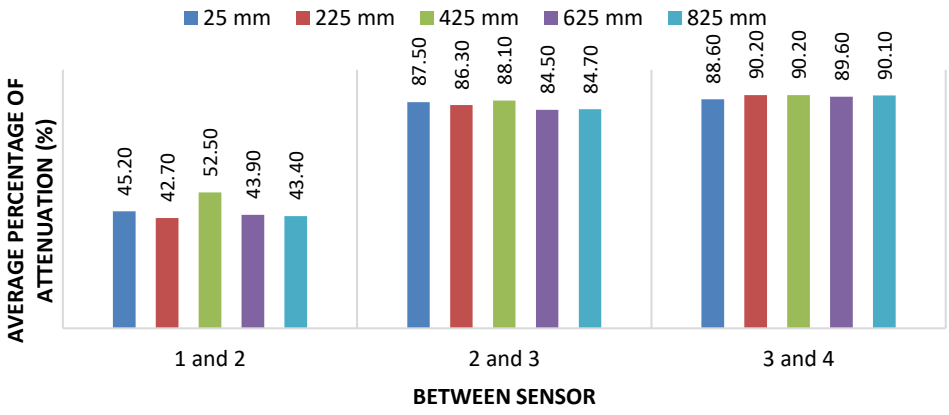

Figure 4.9: The average percentage of attenuation of concrete with a subsurface crack at different depth.

Figure 4.10 presents the average percentage of attenuation for concrete with different subsurface crack diameters ranging from 100 mm to 500 mm. According to the graph, it can be seen that the average percentage of attenuation between sensor 2 and sensor 3 for concrete with a 100 mm diameter subsurface crack had an average percentage of 84.86 %. In contrast, the average percentage for concrete with a 500 mm diameter subsurface crack was 86.31 %. The average percentage of attenuation increase as the subsurface crack diameter increases. (Lee et al., 2019) conducted a numerical analysis and discovered that a more significant drop in the amplitude index was established from a larger subsurface crack length. Therefore, one can say that a longer subsurface crack will result in a higher percentage of attenuation when the wave propagates through the subsurface crack zone. As the length of the subsurface crack increases, a higher distortion of Rayleigh waves occurs.

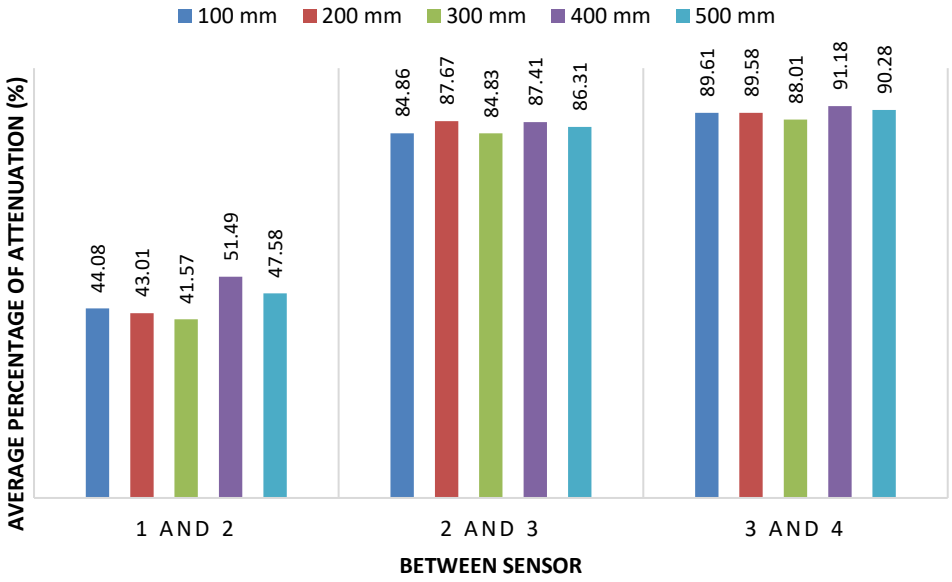

Figure 4.10: The average percentage of attenuation for concrete with different diameters of subsurface cracks.

4.6 Velocity

The distance between sensors and the artificial subsurface crack was set up according to the proposed location, as shown in Figure 3.5 for the Rayleigh wave velocity analysis. The waveforms collected were further analyzed to obtain the propagation velocity of the Rayleigh wave. The velocity of propagation of the Rayleigh wave was determined by dividing the distance

between two sensors by the difference in arrival time between two sensors. The mathematical equation used to determine the Rayleigh wave's propagation velocity was as shown in Equation 4.2.

$$V = \frac{L}{t_{x+1} - t_x}, when\ x = 1, 2, 3 \quad (4.2)$$

where V = Velocity of propagation of Rayleigh wave, m/s,

L = Distance between two sensors, m,

t_{x+1} = Arrival time of Rayleigh wave in the first sensor, s,

t_x = Arrival time of Rayleigh wave in the subsequent sensor, s;

4.6.1 Velocity of the Rayleigh wave

(Liew et al., 2019) states that the average velocity will decrease when the Rayleigh wave propagates through the subsurface crack zone. A lower frequency of wave excitation is more suitable in determining the correlations between the Rayleigh wave's propagation velocity and subsurface crack from the numerical simulations and experimental measurements.

Figure 4.11 – Figure 4.13 represents the velocity profile of concrete specimens with a subsurface crack diameter varying from 100 mm to 500 mm at a depth of 25 mm, 425 mm, and 825 mm obtain from a steel ball with 10 mm, 15 mm, 20 mm, and 25 mm diameters. The typical velocity of elastic waves in air is approximately 343 m/s. The elastic wave's velocity in air is considered instead of an elastic wave in concrete due to the non-contact method adopted in this experimental analysis. From the results obtained, the Rayleigh wave of sound concrete's velocity is 361 m/s, which kept constant from sensor 1 to sensor 4 when propagating through a sound concrete. In contrast, a significant drop of Rayleigh wave velocity was observed from the velocity profile when the Rayleigh wave travels through the subsurface crack zone. Taking the case of the concrete specimen with a subsurface crack of 100 mm diameter at a depth of 25 mm obtained from 20 mm diameter of steel ball, the Rayleigh wave propagation velocity is 396.8 m/s between sensor 1 and sensor 2. After that, a sharp decrease to 310.6 m/s was observed between sensor 2 and sensor 3, and it increased to 396.8 m/s between sensor 3 and sensor 4. A similar decreasing trend of the Rayleigh wave's propagation velocity between sensor 2 and sensor 3 was

also observed from the concrete specimen with a subsurface crack at a depth of 225 mm and 625 mm.

The overall propagation velocity of the Rayleigh wave between sensor 2 and sensor 3 exhibits a velocity lower than the typical velocity of elastic waves in air (343 m/s). It was most likely a result of wave scattering caused by the artificial subsurface crack. The polystyrene board, which acts as the artificial subsurface crack, has a relatively low density. Thus, when the two materials' acoustic impendence has an enormous difference, the wave will be reflected (Lee et al., 2019). It implies that the subsurface crack location could be roughly estimated by observing the propagation velocity between the sensor.

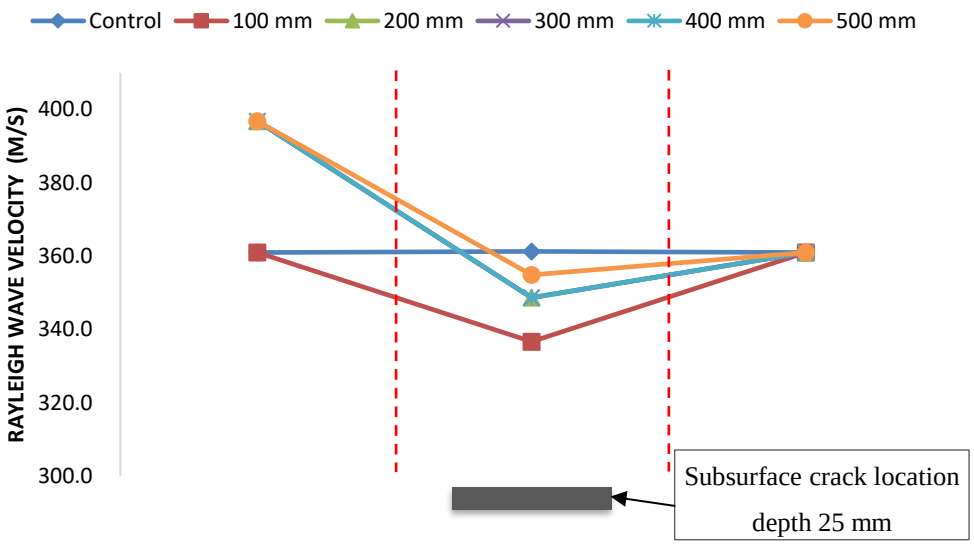

(a)

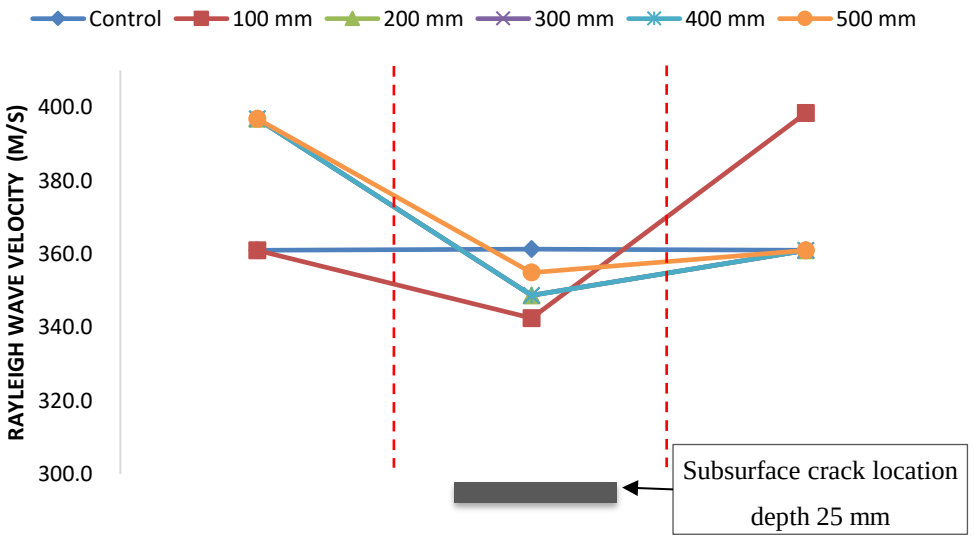

(b)

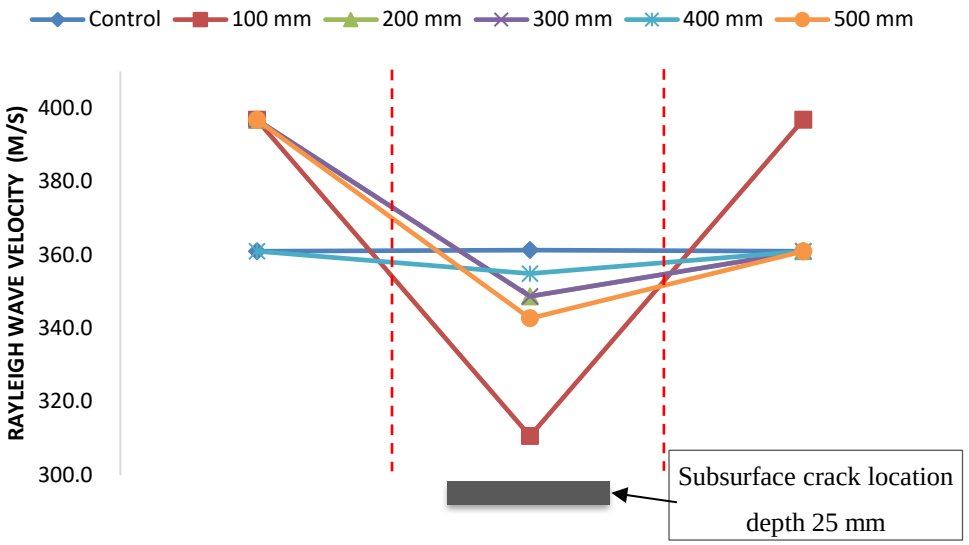

(c)

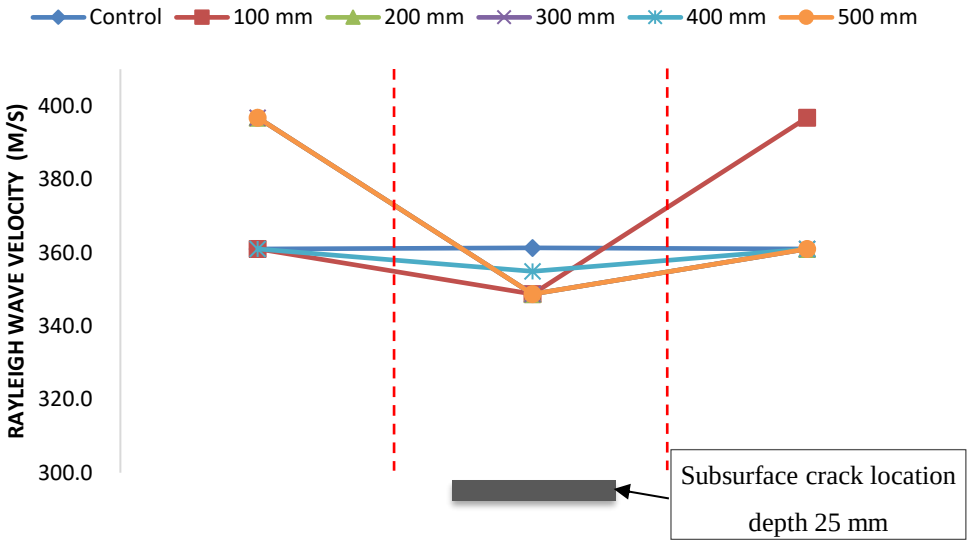

(d)

Figure 4.11: The velocity profile for concrete with a subsurface crack at a depth of 25 mm obtained from a (a) 10 mm diameter steel ball (b) 15 mm diameter steel ball (c) 20 mm diameter steel ball (d) 25 mm diameter steel ball.

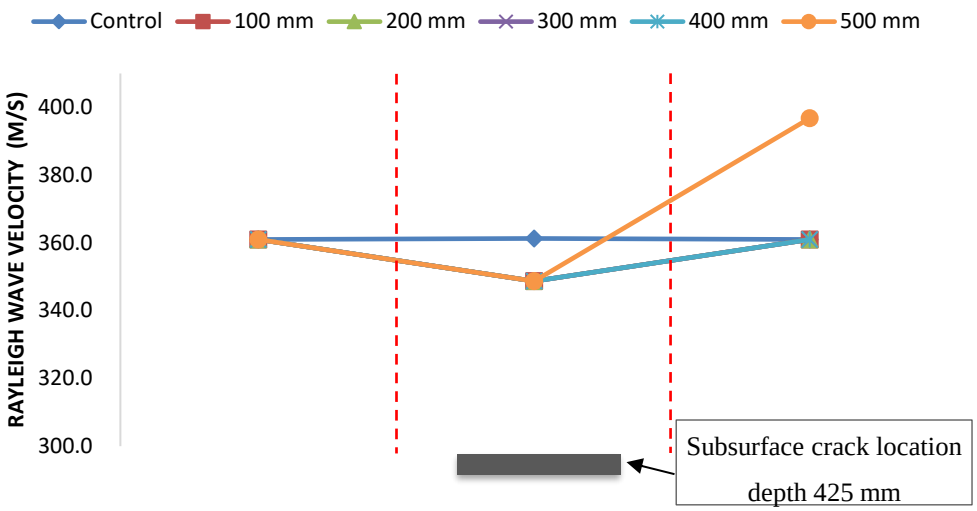
Control
100 mm
200 mm
300 mm
400 mm
500 mm
RAYLEIGH WAVE VELOCITY (M/S)
400.0
380.0
360.0
340.0
320.0
300.0
Subsurface crack location
depth 425 mm

(a)

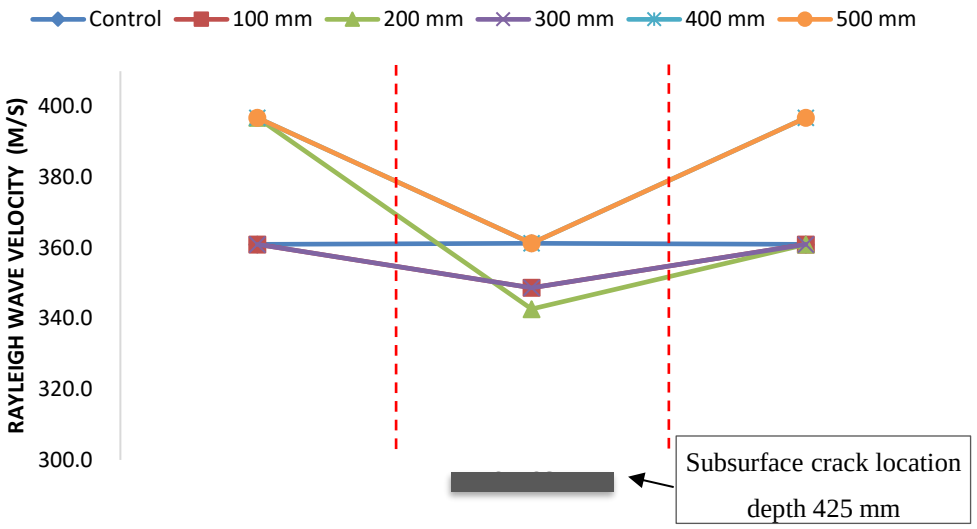
Control
100 mm
200 mm
300 mm
400 mm
500 mm
RAYLEIGH WAVE VELOCITY (M/S)
400.0
380.0
360.0
340.0
320.0
300.0
Subsurface crack location
depth 425 mm

(b)

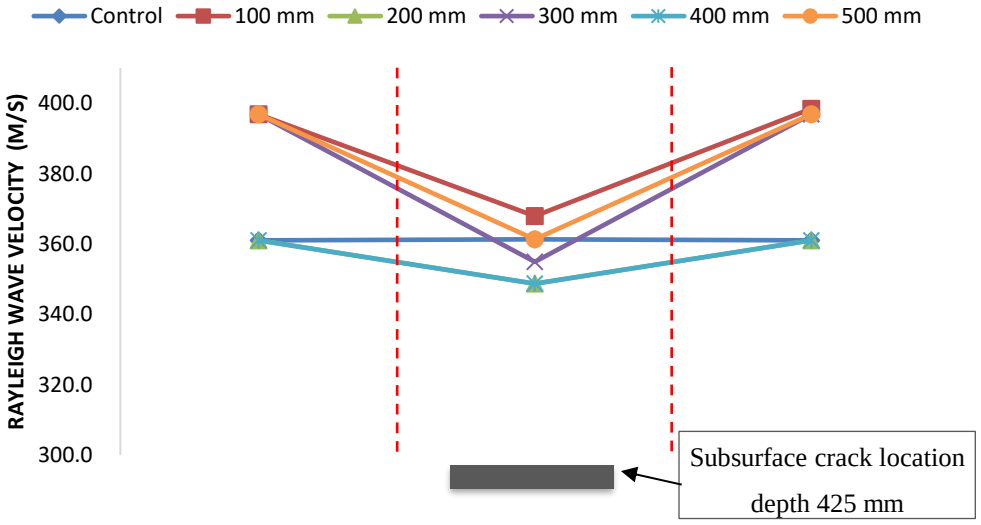
Control
100 mm
200 mm
300 mm
400 mm
500 mm
RAYLEIGH WAVE VELOCITY (M/S)
400.0
380.0
360.0
340.0
320.0
300.0
Subsurface crack location
depth 425 mm

(c)

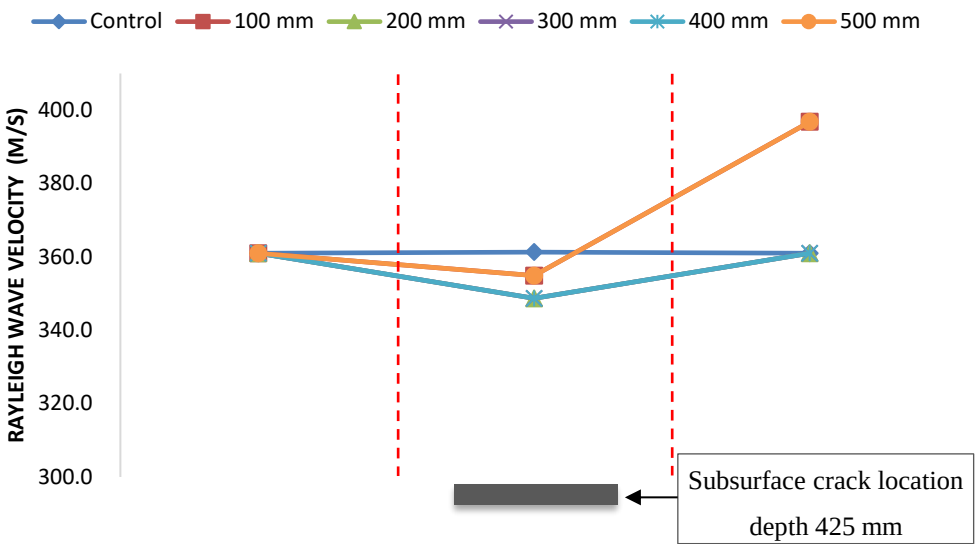

(d)

Figure 4.12: The velocity profile for concrete with a subsurface crack at a depth of 425 mm obtained from a (a) 10 mm diameter steel ball (b) 15 mm diameter steel ball (c) 20 mm diameter steel ball (d) 25 mm diameter steel ball.

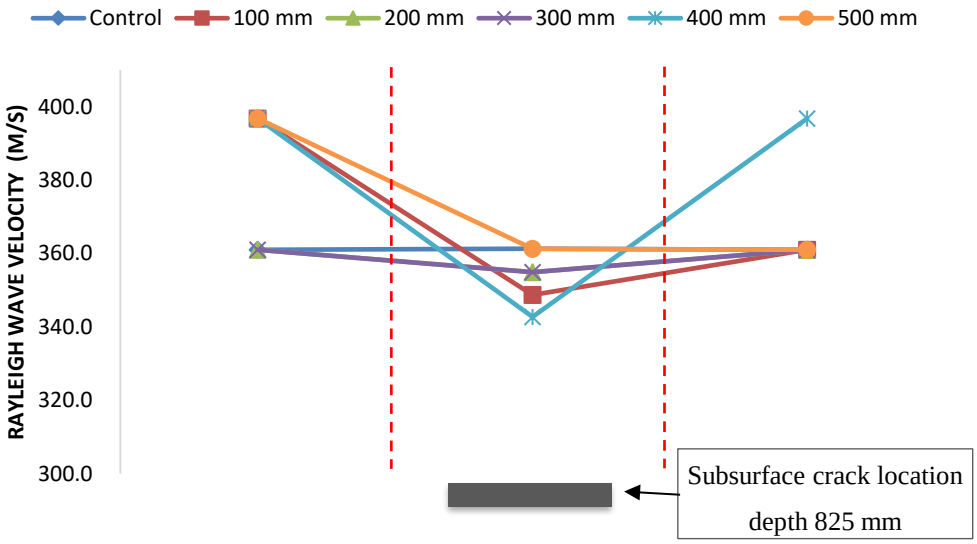

(a)

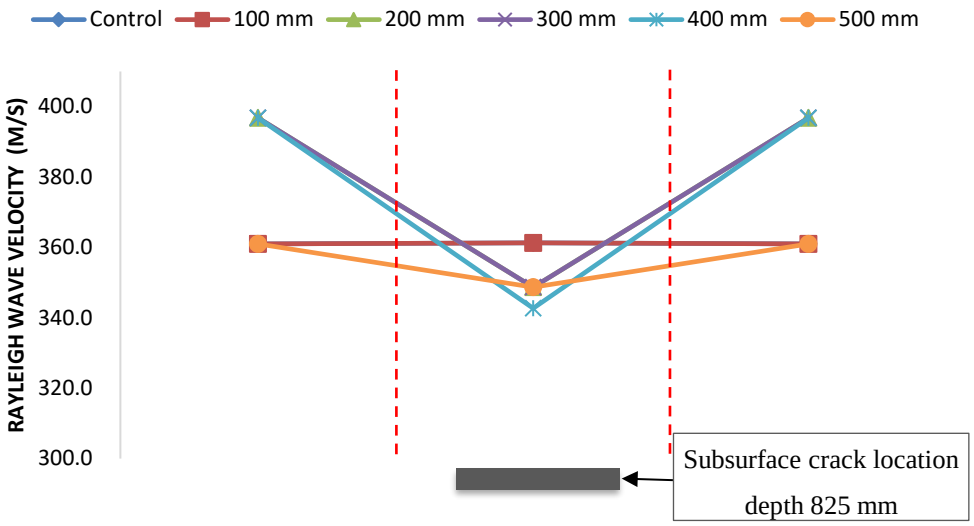
Control
100 mm
200 mm
300 mm
400 mm
500 mm
RAYLEIGH WAVE VELOCITY (M/S)
400.0
380.0
360.0
340.0
320.0
300.0
Subsurface crack location
depth 825 mm

(b)

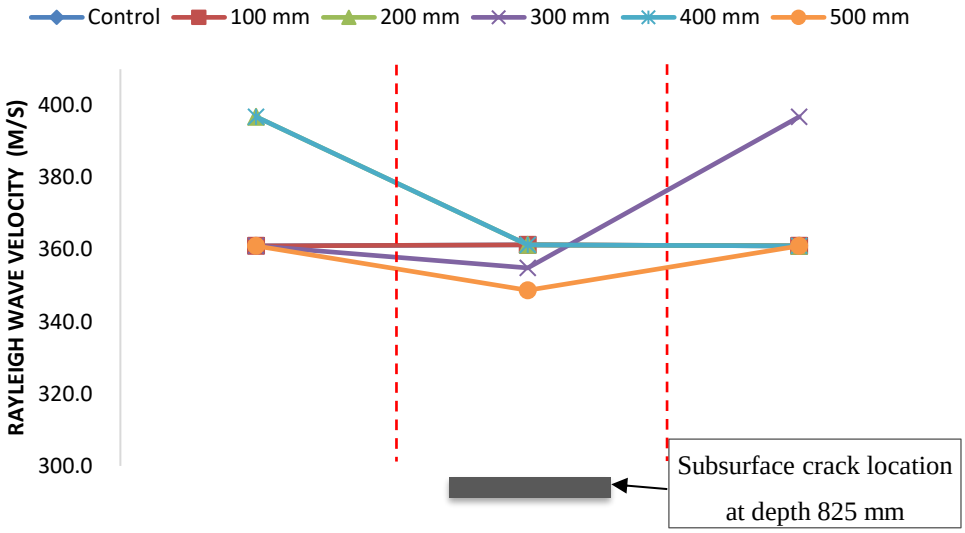
Control
100 mm
200 mm
300 mm
400 mm
500 mm
RAYLEIGH WAVE VELOCITY (M/S)
400.0
380.0
360.0
340.0
320.0
300.0
Subsurface crack location
at depth 825 mm

(c)

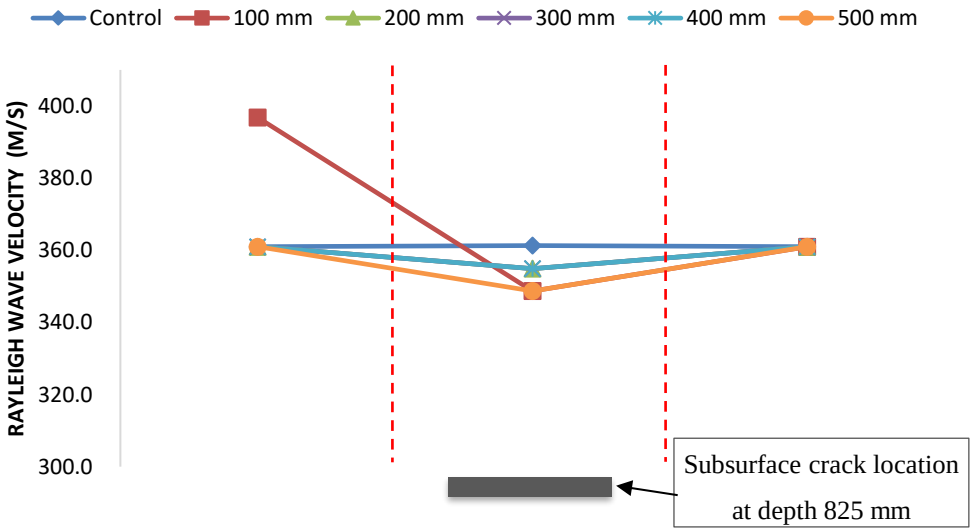
Control
100 mm
200 mm
300 mm
400 mm
500 mm
RAYLEIGH WAVE VELOCITY (M/S)
400.0
380.0
360.0
340.0
320.0
300.0
Subsurface crack location
at depth 825 mm

(d)

Figure 4.13: The velocity profile for concrete with a subsurface crack at a depth of 825 mm obtained from a (a) 10 mm diameter steel ball (b) 15 mm diameter steel ball (c) 20 mm diameter steel ball (d) 25 mm diameter steel ball.

Table 4.3 presents the percentage difference of average propagation velocity for concrete with a subsurface crack at a depth of 25 mm, 225 mm, 425 mm, 625 mm, and 825 mm obtain from a diameter of steel ball with 10 mm, 15 mm, 20 mm, and 25 mm. The percentage difference of average propagation velocity obtained from steel balls of 10 mm and 25 mm from sensor 2 to sensor 3 were -2.28 % and -3.45 %, respectively. It can be noticed that when the diameter of the steel ball used to generate the elastic waves increases, the percentage difference of average propagation velocity from sensor 2 to sensor 3 also obtained increases. Therefore, it can be said that a lower excitation frequency is more suitable in determining the change of average propagation velocity when propagating through the concrete subsurface crack.

Table 4.3: The percentage difference of average propagation velocity for concrete with a subsurface crack at different depths obtained from different steel ball diameters.

Steel Ball Diameter (mm)	**Depth of Delamination (mm)**	**Percentage difference of average propagation velocity between each sensor (%)**		
		Between sensor 1 to sensor 2	**Between sensor 2 to sensor 3**	**Between sensor 3 to sensor 4**
10	25	7.93	-3.73	0.00
	225	9.92	-0.25	0.00
	425	0.00	-3.41	1.98
	625	5.95	-1.66	7.93
	825	5.95	-2.35	1.98
Average		5.95	-2.28	2.38
15	25	7.93	-3.41	2.07

	225	7.93	-3.05	5.95
	425	5.95	-2.34	3.97
	625	5.95	-2.01	3.97
	825	5.95	-3.04	5.95
Average		6.74	-2.77	4.38
20	25	7.93	-5.51	1.98
	225	3.97	-2.04	5.95
	425	5.95	-1.30	6.04
	625	3.97	-1.31	1.98
	825	3.97	-0.97	1.98
Average		5.16	-2.23	3.59
25	25	5.95	-3.06	1.98
	225	3.97	-2.02	1.98
	425	0.00	-2.72	3.97
	625	5.95	-7.08	1.98
	825	1.98	-2.38	0.00
Average		3.57	-3.45	1.98

Moreover, Figure 4.14 shows the percentage difference of average propagation velocity for concrete with a subsurface crack at different depths ranging from 25 mm to 825 mm. The percentage difference was calculated by using Equation 4.3. According to the graph, it can be seen that the percentage difference of average propagation velocity from sensor 2 to sensor 3 for concrete with a subsurface crack at a depth of 25 mm is -3.93 %. In contrast, the concrete with a subsurface crack at a depth of 825 mm had a percentage difference of -2.19 %. (Lee et al., 2019) conducted a numerical study and found out that a subsurface crack nearer to the concrete's surface exhibited a higher velocity index. Thus, one can say that a deeper subsurface crack is more difficult to be determined in comparison with shallow subsurface cracks. It is most likely due to the limitation of penetration depth of the Rayleigh wave.

$$V\ (\%) = \frac{V_{avg} - V_s}{V_s} \times 100\% \quad (4.3)$$

where $V(\%)$ = Percentage difference of average propagation velocity, %,

V_{avg} = Average propagation velocity between sensors, m/s,

V_s = Propagation velocity of sound concrete, 361 m/s.

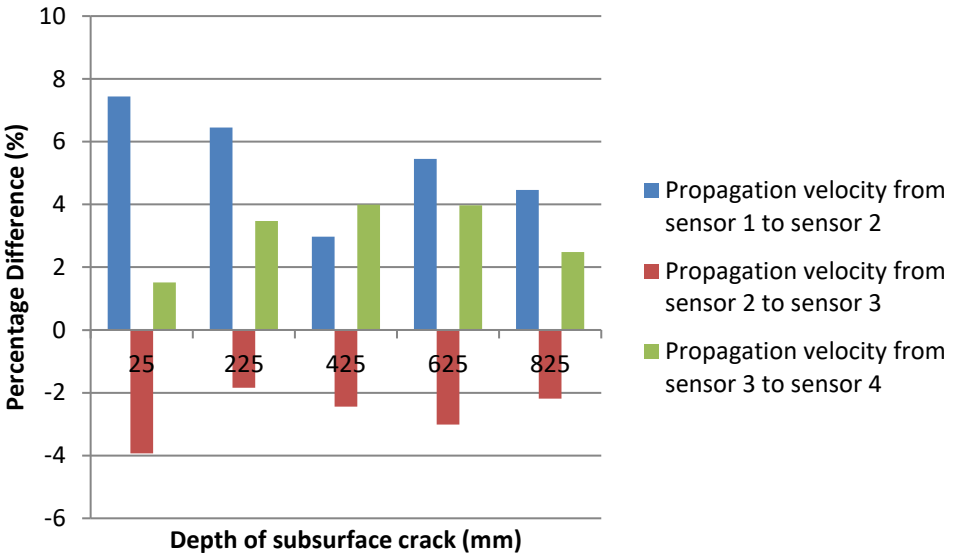

Figure 4.14: The percentage difference of average propagation velocity of concrete with a subsurface crack at different depths.

Figure 4.15 presents the percentage difference of average propagation velocity of concrete with different subsurface crack diameters ranging from 100 mm to 500 mm. According to the graph, it can be seen that the percentage difference of average propagation velocity from sensor 2 to sensor 3 of the concrete specimen with 100 mm diameter subsurface crack was -3.05 %. In contrast, the percentage difference of average propagation velocity from sensor 2 to sensor 3 of the concrete specimen with 500 mm diameter subsurface crack was -2.01%. Therefore, one can say that a longer subsurface crack is more difficult to be determined in comparison with the shorter subsurface cracks. (Lee et al., 2019) stated that the velocity index would be affected by the length of the subsurface crack, where a lower velocity index will be obtained from a longer subsurface crack.

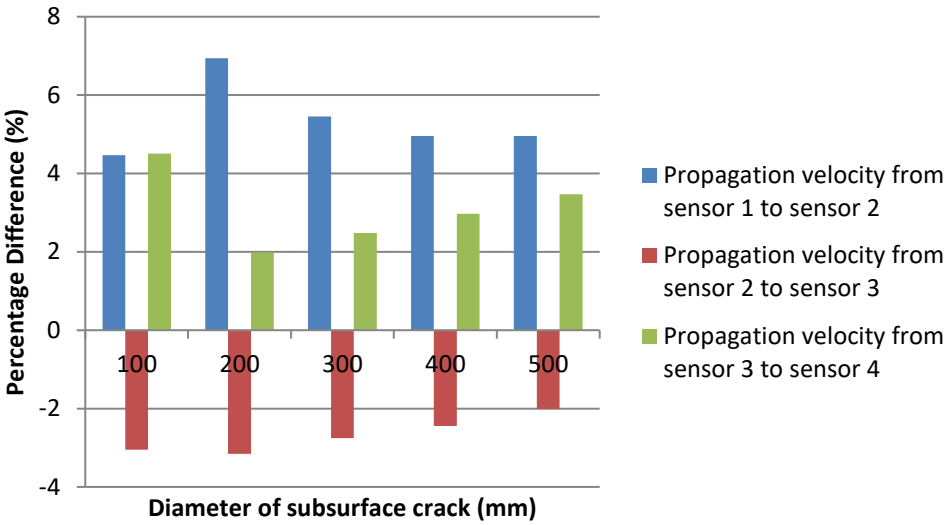

Figure 4.15: The percentage difference of average propagation velocity for concrete with different subsurface crack diameters.

4.7 Fast Fourier Transform (FFT)

FFT is in the order of N log N, where N is known as the data size. The FFT algorithm is almost linear in N, and it has a slight correction of log N in the scaling. Therefore, log N will become less significant when N is a considerable value. FFT is beneficial for real signal audios and images. In this research study, the Rayleigh wave can be separated from the other waves by applying the FFT algorithm using software called MATLAB®. This algorithm was used to convert waveforms between the time domain and frequency domain.

4.7.1 Frequency domain analysis

By applying the Fast Fourier transform, the frequency component can be converted from the time function. For a frequency domain graph, the amplitude was plotted versus a range of frequencies. The time-domain graph and frequency domain graph is shown in Figure 4.16. From the frequency domain graph, it can be noticed that the maximum frequency represents the arrival of the Rayleigh wave, which is extracted from the initially collected waveforms.

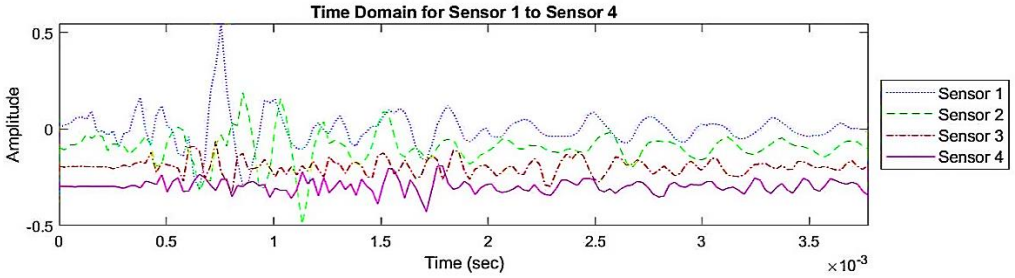

(a)

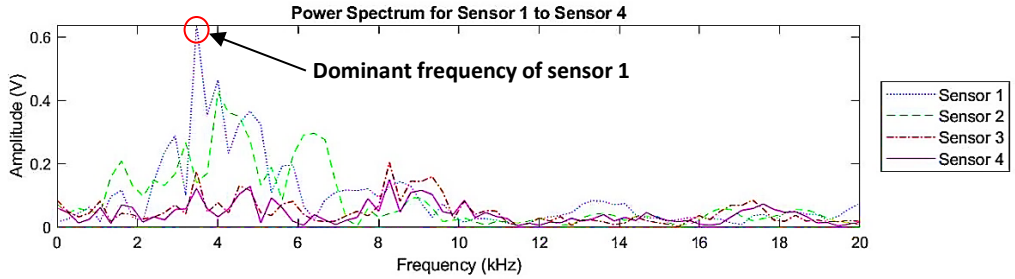

(b)

Figure 4.16: Waveform collected which was plotted using MATLAB® (a) Time domain graph (b) Frequency domain graph.

4.7.2 Dominant frequency of the Rayleigh wave

The Rayleigh wave's dominant frequency can effectively determine the presence and location of the concrete subsurface crack. (Liew et al., 2019) conducted a numerical analysis and stated that the dominant frequencies for the higher excitation frequencies would decrease when the Rayleigh wave's propagation approaches the subsurface crack zone. On the other hand, the peak frequencies will remain unchanged for the lower frequency excitations.

Figure 4.17 represents the dominant frequency for concrete with different subsurface crack diameters ranging from 100 mm to 500 mm at different depths, obtained from 10 mm and 15 mm diameter of steel ball. From the results obtained, a significant drop of the dominant frequency at sensor 2 was noticed. The decreasing trend was seen in sensor 2 because the artificial subsurface cracks were located between sensor 2 and sensor 3. By comparing the dominant frequency graph of 100 mm and 500 mm subsurface crack diameter, it can be noticed that the decreasing trend at sensor 2 increases as the crack diameter increases. It can prove that a longer crack can result in a more significant drop of dominant frequency at sensor 2.

The dominant frequency of the Rayleigh wave at sensor 2 exhibits the lowest peak among the 4 sensors. The primary reason for this phenomenon is the inhomogeneity of the artificial subsurface crack with the concrete that causes the reflection of an extensive amount of elastic wave energy. When the artificial subsurface crack's inhomogeneity increases, the tendency of geometric spreading of the Rayleigh wave increases.

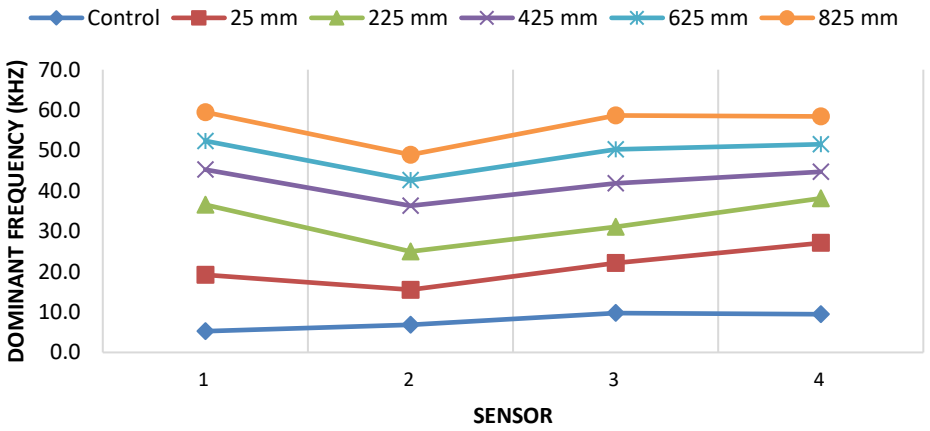

(a)100 mm subsurface crack diameter obtained from 15 mm diameter of steel ball.

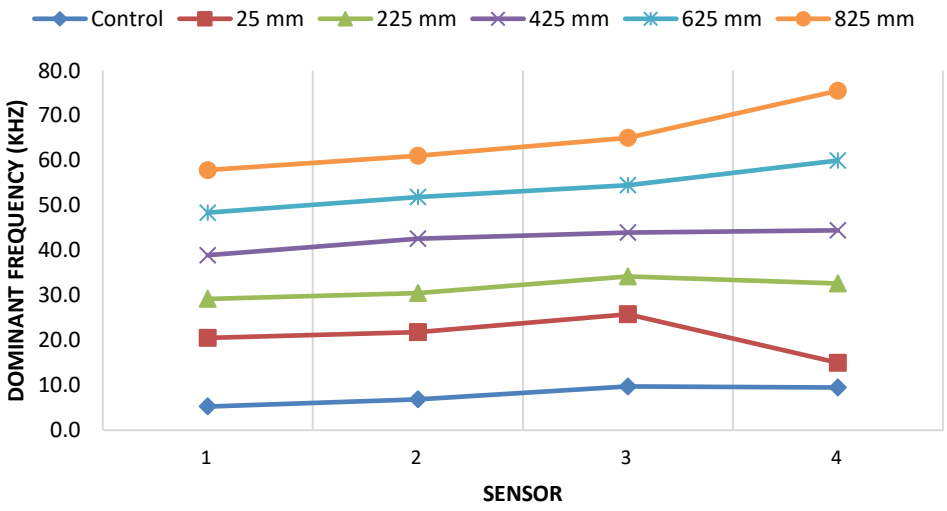

(b) 200 mm subsurface crack diameter obtained from 10 mm diameter of steel ball.

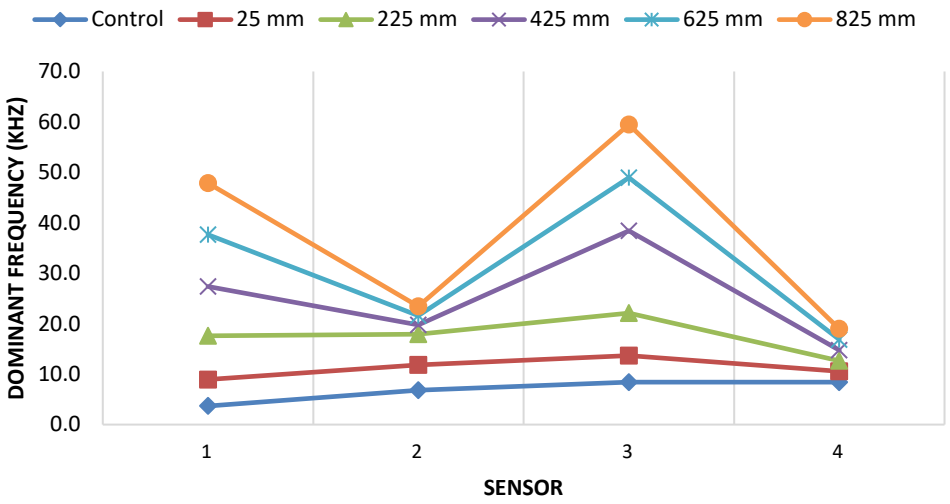

(c) 300 mm subsurface crack diameter obtained from 15 mm diameter of steel ball.

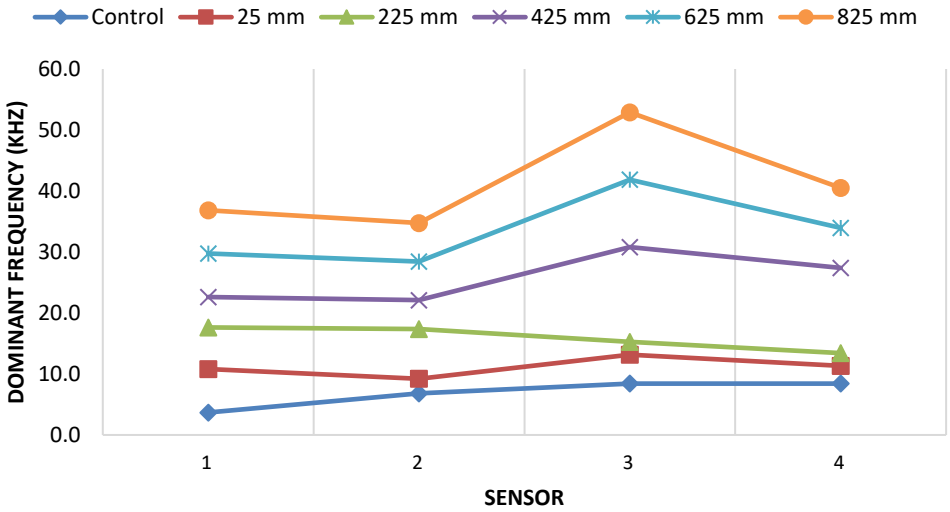

(d) 400 mm subsurface crack diameter obtained from 15 mm diameter of steel ball.

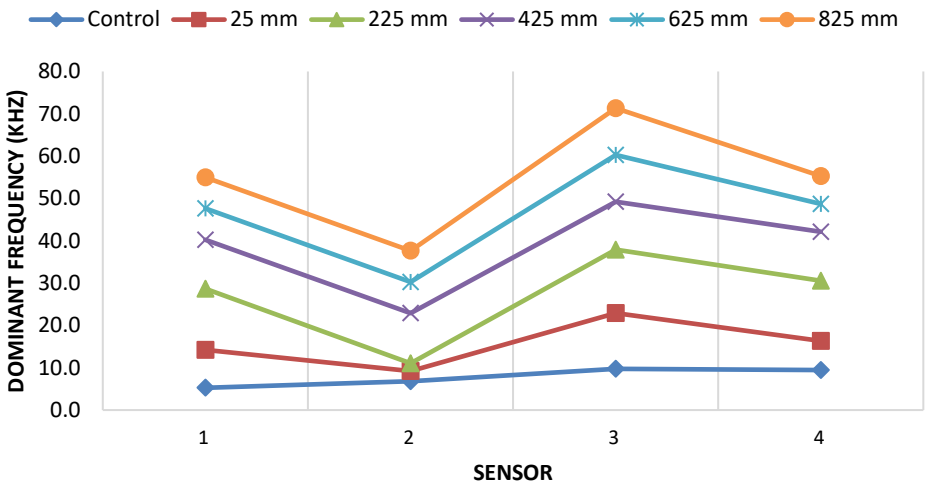

(e) 500 mm subsurface crack diameter obtained from 10 mm diameter of steel ball.

Figure 4.17: The peak frequency for concrete with different subsurface crack diameters obtained from different steel ball diameters.

Figure 4.18 represents the dominant frequency for concrete with different diameters of subsurface crack at a depth ranging from 25 mm to 825 mm obtained from 10 mm and 15 mm diameter of steel ball. From the graphs obtained, a drop of the dominant frequency at sensor 2 was noticeable. It was most likely due to the artificial subsurface cracks located between sensor 2 and sensor 3. From the results obtained by (Liew et al., 2019) in the numerical simulation, a shifting trend in Reciever 2 is observed for the top subsurface crack, where the subsurface crack is located between sensor 2 and sensor 3. By comparing the dominant frequency graph of a subsurface crack at depths of 25 mm and 825 mm, it can be noticed that the decreasing trend at sensor 2 becomes less significant as the crack depth increases. When the subsurface cracks' depth increase, the decreasing trend at sensor 2 was noticeable only for the longer crack. This finding shows that the dominant frequency had a minimum effect for a deeper crack. The deeper crack had fewer effects on the peak frequency as Rayleigh wave penetration depth was restricted to one wavelength depth.

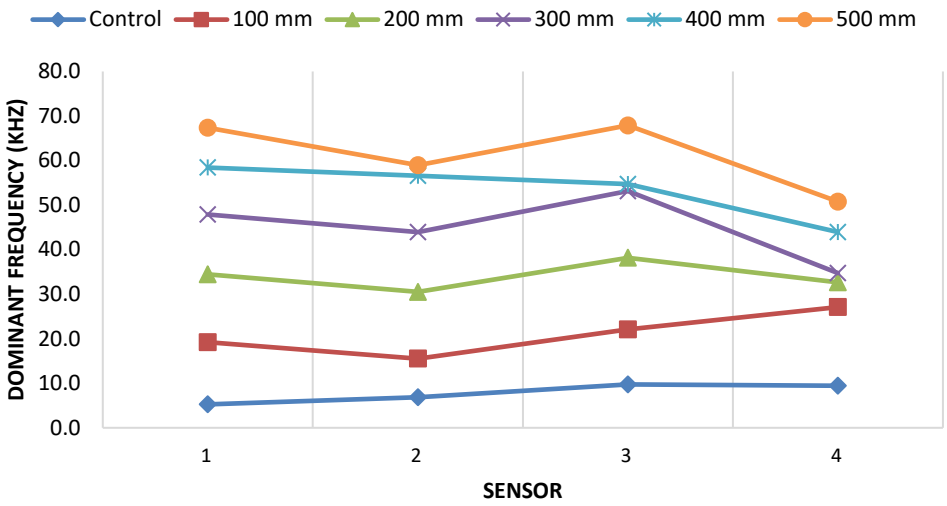

(a) subsurface crack at depth of 25 mm obtained from 15 mm diameter of steel ball.

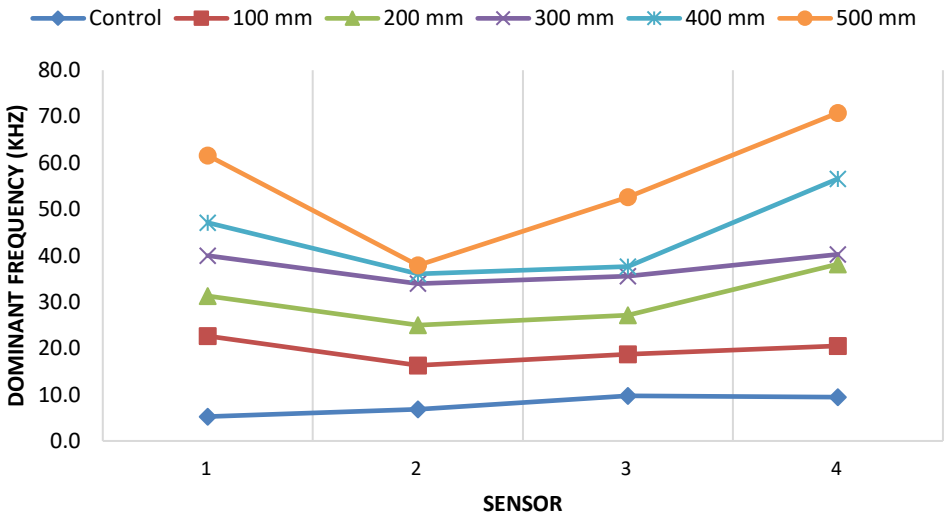

(b) subsurface crack at depth of 225 mm obtained from 15 mm diameter of steel ball.

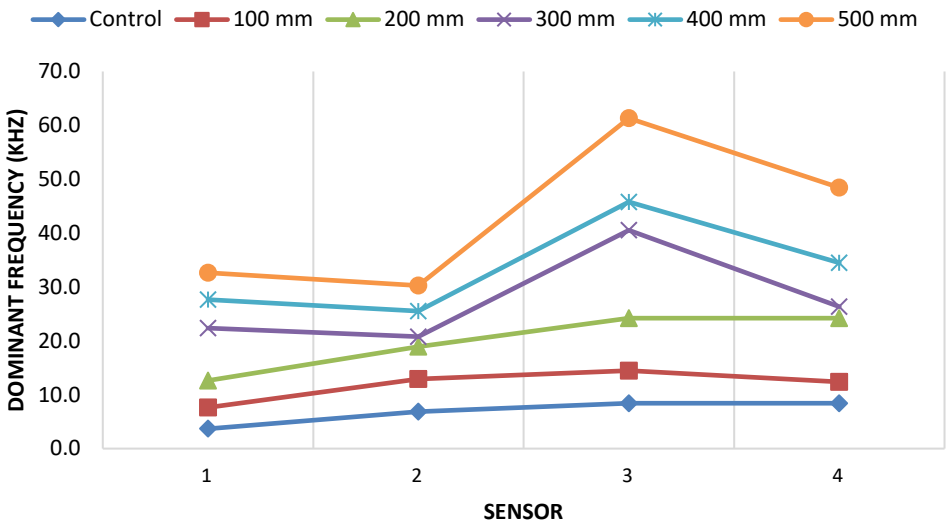

(c) subsurface crack at depth of 425 mm obtained from 15 mm diameter of steel ball.

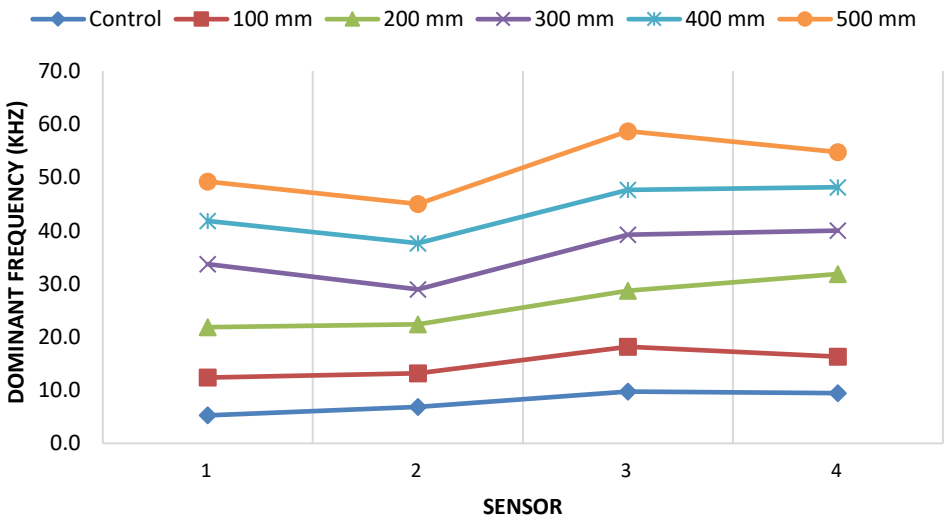

(d) subsurface crack at depth of 625 mm obtained from 15 mm diameter of steel ball.

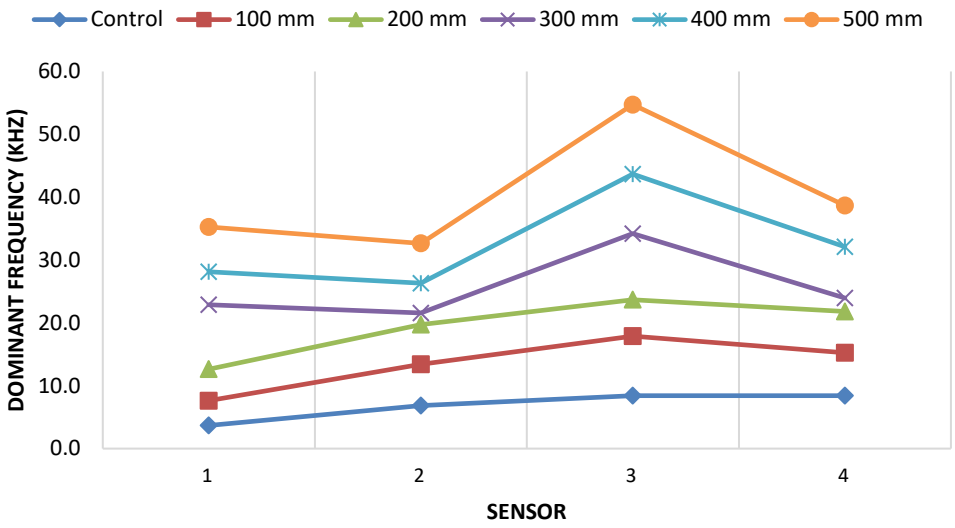

(e) subsurface crack at depth of 825 mm obtained from 15 mm diameter of steel ball.

Figure 4.18: The peak frequency for concrete with a subsurface crack at different depth.

The diameter of steel balls with 10 mm, 15 mm, 20 mm, and 25 mm were used to generate Rayleigh waves in different frequencies in this experiment. The correlation of Rayleigh wave with dominant frequency in this research study does not show a consistent trend when varying the use of different steel ball diameters. But it can be noticed that more remarkable results were obtained from a smaller diameter steel ball. When the steel ball's diameter used to generate the elastic waves decreases, the higher the Rayleigh wave frequency. The frequency is proportional to the wavelength. The longer the wavelength, the deeper the depth of penetration of the Rayleigh wave. Therefore, it can be said that a higher excitation frequency is more suitable in determining the change in peak frequency when the concrete subsurface crack exists.

4.8 Summary

In this experimental study, the Rayleigh wave's arrival time is characterized by a strong peak in the amplitude which appears after the first arrival of the longitudinal wave, which can be observed from the time-domain graph. The delay in the Rayleigh peak was noticed when a subsurface crack exists. When the steel ball's diameter used to generate elastic waves increases, the

waveforms' amplitude increases, making it easier to be determined. The increases in diameter of the steel ball show the decrease of frequency generated. Amplitude is inversely proportional to the frequency. When the diameter of the subsurface crack increases, the delay in the Rayleigh peak slightly increases. The weaker waveform amplitude was detected when the depth of subsurface crack increases.

Attenuation refers to the decay in the amplitude of the wave. This phenomenon can effectively determine the presence of a subsurface crack. The amplitude of the Rayleigh waves sharply decreases when the Rayleigh wave travels through the subsurface crack zone. Attenuation increase when the diameter of the steel ball decreases. It indicates that attenuation increase with the frequency of wave generated. When the diameter of the subsurface crack increases, the attenuation increase. The attenuation is minor when the location of the subsurface crack is deeper.

Furthermore, the method used in this research study was the non-contact method. From the results obtained, the velocity of the Rayleigh wave of sound concrete is 361 m/s which was constant from sensor 1 to sensor 4. The results obtained were tally with the typical velocity of elastic waves in air (343 m/s). A significant decline of the Rayleigh wave propagation velocity was observed between sensor 2 and sensor 3. The percentage difference of propagation velocity increases when the steel ball diameter increases. Thus, a lower excitation frequency is more suitable to determine the presence of a subsurface crack. When the diameter of the subsurface crack increase, the percentage difference of propagation velocity increases. The change in propagation velocity between sensor 2 and sensor 3 becomes more observable if the subsurface cracks are at a shallower location.

The dominant frequency of the Rayleigh wave can effectively determine the presence of the concrete subsurface crack. From the results obtained, a significant drop in the dominant frequency at sensor 2 was observed. The reduction of dominant frequency at sensor 2 increases when the Rayleigh wave propagates through a longer subsurface crack. Dominant frequency establishes a minor effect for a subsurface crack at a deeper depth. The frequency is proportional to the wavelength. Thus, more remarkable results were obtained from a smaller diameter of steel ball.

Finally, the findings above establish that the Rayleigh wave's attenuation, propagation velocity, and dominant frequency are affected by the artificial subsurface crack. The polystyrene board, which acts as the artificial subsurface crack, causes inhomogeneity between the polystyrene board and the concrete. The presence of artificial subsurface crack causes the scattering and distortion of the Rayleigh wave. The Rayleigh wave has a characteristic where the penetration depth is limited to one wavelength depth. Therefore, the penetration of the Rayleigh wave is less sensitive towards the deep crack. The sensitivity of the Rayleigh wave is higher towards a longer subsurface crack. The inhomogeneity between subsurface crack and concrete increases when the crack diameter increase.

CHAPTER 5

CONCLUSION AND RECOMMENDATIONS

5.1 Introduction

This chapter summarized the results obtained from the experimental study based on the aim and objective proposed in chapter 1. Recommendations were also suggested for improvements of this experimental study and future studies on related topics.

5.2 Conclusion

In this research study, the Rayleigh wave-based non-contact method was conducted to study the correlations of Rayleigh wave amplitude, propagation velocity, and dominant frequency on the concrete subsurface cracks. The concrete subsurface cracks were parallel to the concrete surface at different proposed depths (25 mm, 225 mm, 425 mm, 625 mm, and 825 mm) and different crack diameters (100 mm, 200 mm, 300 mm, 400 mm, and 500 mm). The Rayleigh wave was generated using various diameters of steel balls (10 mm, 15 mm, 20 mm, and 25 mm) to characterize the concrete subsurface cracks.

This research study's first objective is to determine the Rayleigh wave characteristics' changes when propagating through a sound concrete and concrete with a subsurface crack. According to the experimental analysis results, the conclusions are drawn as shown below:-

1. A delay in the Rayleigh peak's arrival time can be noticed from the time domain graph when there is a presence of a subsurface crack.
2. The delay in the Rayleigh peak's arrival time becomes more significant when the subsurface cracks diameter increases.
3. The delay in the Rayleigh peak's arrival time becomes less evident when the subsurface cracks depth increases.

This research study's second objective is to determine the Rayleigh wave's properties when propagating through concrete with different diameters and different depths of subsurface cracks, namely the attenuation, the velocity

of propagation, and the dominant frequency. According to the experimental analysis results, the conclusions are drawn as shown below:-

1. An enormous decay in the amplitude was observed between sensor 2 and sensor 3, where the artificial subsurface crack was between them. The average percentage of attenuation increases when the subsurface cracks diameter increases. The average percentage of attenuation decreases when the subsurface cracks at a deeper location.
2. The sharp decreasing trend of the propagation velocity was observed between sensor 2 and sensor 3, where the artificial subsurface crack was between them. The average percentage change of propagation velocity between sensor 2 and sensor 3 reduces when the subsurface cracks diameter and depth increase.
3. A drop in dominant frequency was observed at sensor 2, where the artificial subsurface crack was between sensor 2 and sensor 3. The increase in the diameters of subsurface crack will result in a more significant drop of dominant frequency at sensor 2. The reduction in dominant frequency in sensor 2 becomes less significant when the depth of subsurface crack increases.

This research study's third objective is to compare the waveforms result obtained when 10 mm, 15 mm, 20 mm, and 25 mm diameter of steel ball used to generate Rayleigh wave with different frequency. When the steel ball diameter increases, the frequency of wave generated decreases. According to the experimental analysis results, the conclusions are drawn as shown below:-

1. The amplitude of waveforms obtained from the time domain graph becomes more significant when the steel ball's diameter increases. The amplitude of the wave is inversely proportional to the frequency of the wave.
2. The average percentage of attenuation increases when the steel ball diameter reduces. The average percentage of attenuation is inversely proportional to the frequency of the wave.
3. The Rayleigh wave propagation velocity increases when the steel ball diameter increases. The propagation velocity of the wave is proportional to the frequency of the wave.

4. The drop of dominant frequency in sensor 2 obtained from a smaller steel ball diameter was more remarkable.

In a nutshell, the conclusion drawn above established that the Rayleigh wave's propagation is affected by the artificial concrete subsurface crack. The polystyrene board acting as the artificial subsurface crack causes the inhomogeneity between the polystyrene board and the concrete. Polystyrene board has a lower acoustic impedance compared to concrete. When the acoustic impedance between two materials is high, the scattering and distortion of the Rayleigh wave will occur. The penetration depth of the Rayleigh wave is also limited to one wavelength depth. Thus, the penetration of the Rayleigh wave is less sensitive towards the deep crack. The sensitivity of the Rayleigh wave is higher towards a longer subsurface crack. The inhomogeneity between subsurface crack and concrete increases when the crack diameter increase.

From the experimental results obtained and conclusion drawn, one can say that the arrival time, percentage of attenuation, the velocity of propagation, and the dominant frequency of a Rayleigh wave are sensitive in detecting the concrete subsurface crack.

5.3 Recommendations

This experimental analysis was carried out with the non-contact-based non-destructive test using the propagation of the Rayleigh wave. The adopted technique can be improved by the recommendations as stated below:-

1. The numerical simulation should be carried out. A comparison should be made between numerical and experimental results to ensure the feasibility of the non-contact-based Rayleigh wave method.
2. The number of sensors used can be increased to illustrate better how the Rayleigh wave behaves when it encounters the subsurface crack.
3. The experimental study should be carried out on different concrete grades and different fiber contents replacement to investigate the Rayleigh wave's properties in various concrete types.

4. The concrete subsurface crack should be created using the 4-point bending technique as concrete delamination will be formed randomly in real life. The results between both ‘real’ subsurface crack and the ‘artificial’ subsurface crack should be compared to understand better the correlation of Rayleigh wave properties on concrete subsurface cracks.

REFERENCES

Aggelis, D., Leonidou, E. and Matikas, T., 2012. Subsurface crack determination by one-sided ultrasonic measurements. *Cement and Concrete Composites*, 34(2), pp.140-146.

Aggelis, D., Kordatos, E., Strantza, M., Soulioti, D. and Matikas, T., 2011. NDT approach for characterization of subsurface cracks in concrete. *Construction and Building Materials*, 25(7), pp.3089-3097.

Blitz, J. and Simpson, G., 1996. *Ultrasonic Methods Of Non-Destructive Testing*. London: Chapman & Hall.

CADENCE. 2018. *Time Domain Analysis vs Frequency Domain Analysis: A Guide and Comparison.* [online] Available at: <https://resources.pcb.cadence.com/blog/2020-time-domain-analysis-vs-frequency-domain-analysis-a-guide-and-comparison#:~:text=As%20stated%20earlier%2C%20a%20time,concerning%20a%20range%20of%20frequencies.> [Accessed 27 February 2021].

Chakravarthi, B., 2014. *Study On Different Types Of Cracks In Plain And Reinforced Concrete*. [online] Research Gate. Available at: <https://www.researchgate.net/publication/286601793_STUDY_ON_DIFFERENT_TYPES_OF_CRACKS_IN_PLAIN_AND_REINFORCED_CONCRETE> [Accessed 28 August 2020].

Chakraborty, J., Katunin, A., Klikowicz, P. and Salamak, M., 2019. Early Crack Detection of Reinforced Concrete Structure Using Embedded Sensors. *Sensors*, 19(18), p.3879.

Dagher, H. J., and Kulendran, S. _1992_. “Finite element modelling of corrosion damage in concrete structures.” *ACI Struct. J.*, 89_6_, 699–709.

Endsley, K., 2007. *What Is Seismology And What Are Seismic Waves?*. [online] Geo.mtu.edu. Available at: <http://www.geo.mtu.edu/UPSeis/waves.html> [Accessed 18 August 2020].

Eraky, A., Samir, R., El-Deeb, W. and Salama, A., 2018. DETERMINATION OF SURFACE AND SUB-SURFACE CRACKS LOCATION IN BEAMS

USING RAYLEIGH-WAVES. *Progress In Electromagnetics Research C*, 80, pp.233-247.

Ghosh, D., Beniwal, S., Ganguli, A. and Mukherjee, A., 2018. Reference free imaging of subsurface cracks in concrete using Rayleigh waves. *Structural Control and Health Monitoring*, 25(10), p.e2246.

Giatec Scientific Inc. 2019. *Evaluating Cracking In Concrete: Procedures | Giatec Scientific Inc.*. [online] Available at: <https://www.giatecscientific.com/education/cracking-in-concrete-procedures/> [Accessed 31 August 2020].

In, C., Kim, J., Kurtis, K. and Jacobs, L., 2009. Characterization of ultrasonic Rayleigh surface waves in asphaltic concrete. *NDT & E International*, 42(7), pp.610-617.

Khan Academy. 2020. *Transverse And Longitudinal Waves Review*. [online] Available at: <https://www.khanacademy.org/science/ap-physics-1/ap-mechanical-waves-and-sound/introduction-to-transverse-and-longitudinal-waves-ap/a/transverse-and-longitudinal-waves-ap1> [Accessed 18 August 2020].

Lee, F., Chai, H., Lim, K. and Lau, S., 2019. Concrete Sub-Surface Crack Characterization by Means of Surface Rayleigh Wave Method. *ACI Materials Journal*, 116(1).

Lee, F., Lim, K. and Chai, H., 2015. *Determination and extraction of Rayleigh-waves for concrete cracks characterization based on matched filtering of center of energy*. [online] Science Direct. Available at: <http://dx.doi.org/10.1016/j.jsv.2015.11.004> [Accessed 5 March 2021].

Liew, C., Lee, F., Tan, D., Lim, J., Yew, M. and Woon, Y., 2019. Behavioural study of surface Rayleigh waves in concrete structure containing delamination. *Journal of Civil Structural Health Monitoring*, 9(4), pp.555-564.

Li, C., Zheng, J., Lawanwisut, W. and Melchers, R., 2007. Concrete Delamination Caused by Steel Reinforcement Corrosion. *Journal of Materials in Civil Engineering*, 19(7), pp.591-600.

Li, D., Ruan, T. and Yuan, J., 2012. Inspection of reinforced concrete interface delamination using ultrasonic guided wave non-destructive test technique.

Science China Technological Sciences, 55(10), pp.2893-2901.

mailto:www-bgs@bgs.ac.uk, B., 2020. *Seismic Waves | Earthquakes | Discovering Geology | British Geological Survey (BGS)*. [online] Bgs.ac.uk. Available at: <https://www.bgs.ac.uk/discoveringGeology/hazards/earthquakes/seismicWaves.html> [Accessed 18 August 2020].

Mosley, B., Bungey, J. and Hulse, R., 2012. *Reinforced Concrete Design*. 7th ed. New York: Palgrave Macmillan, pp.7-10.

Nde-ed.org. 2019. *Attenuation of Sound Waves*. [online] Available at: <https://www.nde-ed.org/EducationResources/CommunityCollege/Ultrasonics/Physics/attenuation.htm> [Accessed 28 February 2021].

Novotny, O., 1999. *SEISMIC SURFACE WAVES*. [online] Geo.mff.cuni.cz. Available at: <http://geo.mff.cuni.cz/vyuka/Novotny-SeismicSurfaceWaves-ocr.pdf> [Accessed 17 August 2020].

Ongpeng, J., Oreta, A. and Hirose, S., 2018. Contact and Noncontact Ultrasonic Nondestructive Test in Reinforced Concrete Beam. *Advances in Civil Engineering*, 2018, pp.1-10.

Physicsclassroom.com. 2020. *Physics Tutorial: What Is A Wave?*. [online] Available at: <https://www.physicsclassroom.com/class/waves/Lesson-1/What-is-a-Wave#:~:text=Waves%20involve%20the%20transport%20of,another%20location%20without%20transporting%20matter.> [Accessed 19 August 2020].

Schabowicz, K., 2019. Non-Destructive Testing of Materials in Civil Engineering. *Materials*, 12(19), p.3237.

Sciencedirect.com. 2020. *Elastic Wave - An Overview | Sciencedirect Topics*. [online] Available at: <https://www.sciencedirect.com/topics/engineering/elastic-wave#:~:text=10.11.&text=According%20to%20elastic%20wave%20theory,wave%20velocity%20is%20in%20between.&text=Under%20normal%20conditions%2C%20cracks%20rarely,before%20they%20curve%20or%20branch.> [Accessed 18 August 2020].

Seismicresilience.org.nz. 2020. *Surface Waves » Seismic Resilience*. [online] Available at: <http://www.seismicresilience.org.nz/topics/seismic-science-and-site-influences/earthquake-energy/surface-waves/> [Accessed 18 August 2020].

Yilmaz, B., Asokkumar, A., Jasiūnienė, E. and Kažys, R., 2020. Air-Coupled, Contact, and Immersion Ultrasonic Non-Destructive Testing: Comparison for Bonding Quality Evaluation. *Applied Sciences*, 10(19), p.6757.